PREDICTION OF MOISTURE TRANSFER IN MIXTURES OF SOLIDS: TRANSFER VIA THE VAPOR PHASE

BY

GEORGE P. GRANDOLFI

(under the supervision of Professor George Zografi)

A thesis submitted in partial fulfillment of the requirements for the degree of

MASTER OF SCIENCE

(PHARMACY)

at the

UNIVERSITY OF WISCONSIN-MADISON

1987

ACKNOWLEDGEMENTS

I would like to extend my deepest appreciation to Professor George Zografi who has skillfully guided me in my academic endeavors while here at the University of Wisconsin. These brief words cannot begin to express my gratitude to Dr. Zografi who, through his enthusiasm for science and dedication to students, has provided me with constant motivation throughout the duration of this work. He is an outstanding academician and a true gentleman. It has been my sincere pleasure working with Professor Zografi.

Additionally, I am particularly grateful to the following:

Dr. Mark J. Kontny for his ideas and suggestions at the onset of this project as well as his continuing thoughts throughout its duration,

Dr. Douglas W. Mendenhall for his support and encouragement in this area of research, and

William H. Rorer Company for the financial support provided to fund this research project.

Finally, I wish to express a special thanks to my parents who have given unending moral support during the past several years, and to Ann Waldbillig who on countless occasions provided strength and instilled courage. Their caring efforts have hardly gone unnoticed.

TABLE OF CONTENTS

LIST OF TABLES

LIST OF FIGURES

I. INTRODUCTION

A. The Effect of Moisture on Pharmaceutical Solids

The interaction of water with pharmaceutical solids occurs in virtually all stages of manufacture, from synthesis of raw materials to storage of the final dosage form. This water may arise from several sources, such as:

1) water vapor sorbed[1] from environmental surroundings;

2) water introduced during processing procedures such as; wet granulation, spray drying, lyophilization or freeze-drying, and aqueous film coating procedures; and

3) formation of crystal hydrates.

The different components which comprise a solid dosage form can vary considerably in their respective capacities to hold water. For example, microcrystalline cellulose at 6%, corn starch at 12%, and gelatin capsules at 18% are approximate water content values which might be expected

[1] Uptake onto the surface of a solid is generally defined as *ad*sorption, while uptake into a solid structure is generally defined as *ab*sorption. When both processes occur the term sorption is used. Since most of the excipients used in pharmaceutical systems take water vapor up by both adsorption and absorption, the general term sorption will be used throughout this thesis when referring to the uptake of water vapor by solids.

when storage of these materials is maintained at about 50% relative humidity. The moisture in a final product may arise from three sources:

1) moisture initially introduced with the individual components;

2) moisture present in the vapor state within the product container; and

3) if the container allows permeation of water vapor, moisture which may enter or leave through the container.

Both physical and chemical properties of a finished product may be affected by the moisture content of components in the formulation. Several examples describing water's effect on physical and chemical properties follow.

Van Campen, Amidon, and Zografi (1) have reviewed the background for the phenomenon of deliquescence of solids, whereby a water-soluble drug substance may become dissolved in moisture taken up from the environment. Any water-soluble solid has a critical relative humidity, RH_o, characteristic of the solid and equal to the equilibrium water vapor pressure over a saturated solution of the solid, above which deliquescence will occur. Suppose a solid was placed in some atmospheric relative humidity, RH_i, such that

water vapor adsorbed onto the surface of the solid. This would produce a film saturated with dissolved solid. If RH_i was above the RH_o of the solid, then further uptake would occur because of the vapor pressure difference causing solid to dissolve and to saturate this surface film. This would maintain the relative humidity at the surface at RH_o. Equilibrium eventually would be established with RH_i once total dissolution of the solid and some degree of solution dilution had occurred.

Moisture may also affect flow properties and compaction characteristics of powders. Armstrong and Griffiths (2) showed that the presence of moisture caused a deterioration of powder and granule flow properties due to increased internal cohesion between particles. Hiestand (3), however, indicated that the presence of some moisture could aid granule flow by providing sufficient surface conductivity to reduce the electrostatic charge on the particles. Armstrong and Griffiths also suggested that during compaction high moisture contents should cause adhesion of powders to punch faces, whereas lamination of tablets would be expected with low moisture contents. This latter suggestion was supported by Tabibi (4) with

compressible sugar and by Huttenrauch and Jacob (5) with microcrystalline cellulose. Zografi and Kontny (6), using these data, showed that a reduction of sorbed water just below the amount necessary for a single molecular layer of coverage was enough to impair the direct compaction characteristics of these materials.

Khan, Musikabhumma, and Warr (7) examined the effects on various tablet properties due to different moisture levels of microcrystalline cellulose included in the formulation. It was shown that an increased crushing strength was achieved as the moisture content of the microcrystalline cellulose was increased from 0.9% to 7.3%. Times for disintegration and 90% dissolution, likewise, increased due to increased tablet strength and reduced tablet porosity. The reduced tablet porosity apparantly causes a decreased penetration of water into the tablet structure. Many other studies have examined the effects of water on the crushing strength of tablets. Nakabayashi, Shimamoto, and Mima (8), for example, studied the crushing strength of lactose-corn starch tablets. In all instances, the crushing strength decreased as the moisture content was increased over the range of 22% to 82% relative humidity. Shotton and Rees (9,10), Down and McMullen (11), and Lordi

and Shiromani (12,13) in work with compacts of water-soluble salts showed an increase in crushing strength with an increase in water content. Shotton and Rees attributed this increase to recrystallization of high energy crystal lattice defects in the presence of moisture imparted during the compaction process.

Chemical degradation of a drug via hydrolytic processes in the presence of moisture is another concern of primary importance. In 1958, Leeson and Mattocks (14) studied the hydrolytic decompostion of aspirin in the presence of moisture. In treating their data, two fundamental assumptions were proposed: a) multiple layers of water were adsorbed onto the aspirin surface in an amount dependent on the water vapor pressure, and b) this water film rapidly formed a saturated solution of drug dissolved from the surface. Decomposition then occurred by acid-catalyzed hydrolysis. These workers were able to provide a kinetic model for aspirin degradation which made it possible to adequately predict the stability of aspirin under known conditions of temperature and humidity. Carstensen and Pothisiri (15) showed similar decomposition patterns for p-aminosalicylic acid in the presence of very low moisture. Their data supported the sorbed moisture

theory of Leeson and Mattocks.

Another stability study using aspirin was performed by Manudhane, Contractor, Kim, and Shangraw (16). These researchers investigated decomposition of aspirin tablets which had been formulated with one of the following fillers: microcrystalline cellulose, corn starch, or compressible starch. These excipients provided a range of moisture contents from 5% (microcrystalline cellulose) to 12% (compressible starch). It was found that the decomposition of aspirin by hydrolysis was comparable for all three fillers and hence independent of moisture content. It was suggested that all of the water associated with each excipient, therefore, was not readily available for decomposition of the active ingredient.

Perrier and Kesselring (17) examined the stability of nitrazepam in binary mixtures of various common tablet excipients. These workers hypothesized that the availability of water as a solvent was the important parameter affecting the stability of samples and that the binding energy of water to the excipients was probably the critical factor.

Several reviews have been published concerning the effects of moisture on the stability of solid

pharmaceuticals. Monkhouse (18) reviewed stability problems determined by excipient-drug combinations. It was suggested that the excipient itself was often times inert, but that the water adsorbed onto the excipient surface was the actual reaction component. Carstensen (19) and Monkhouse and Van Campen (20) reviewed several previous theories concerned with water-mediated drug decomposition. Carstensen (21) has applied kinetic equations to the decomposition of solid dosage forms due to excess moisture.

The potential for microbial contamination also must be addressed when moisture is involved. Vos and Labuza (22) suggested that microbial growth was most important when the relative humidity of a food system exceeded 90%.

It is frequently observed that extreme moisture contents, excessive wettness or excessive dryness, are often detrimental to the quality and integrity of the final product. It should thus be a major objective of the pharmaceutical formulator to determine a reasonable final moisture content for a formulation such that an optimization of these physical and chemical properties is achieved. The importance of understanding the effects of water in pharmaceutical solids may be summarized in a statement by Monkhouse (18): "Moisture uptake is perhaps the single most

important factor affecting stability of dosage forms."

B. Vapor Adsorption

Since this thesis is concerned with the transfer of moisture from one component to another via the vapor phase, it is essential to first develop a basic understanding of the vapor adsorption process.

Vapor adsorption studies are most commonly performed at constant temperature giving rise to the familiar isotherm where the amount of vapor adsorbed is plotted as a function of relative vapor pressure. There are several shapes that the isotherm may assume (23,24,25). For many solids commonly utilized in pharmaceutical systems where multilayer physical adsorption occurs, the isotherm is frequently characterized by a sigmoidal shaped curve (Figure 1). As the vapor pressure is progressively increased, molecules adsorb onto the solid adsorbent approaching monolayer formation. It is generally acknowledged that complete monolayer formation is approached somewhere within the early portion of the linear intermediate range of the isotherm. The knee or inflection point is usually used as the value corresponding to this monolayer coverage for calculation purposes. As the vapor pressure is increased further

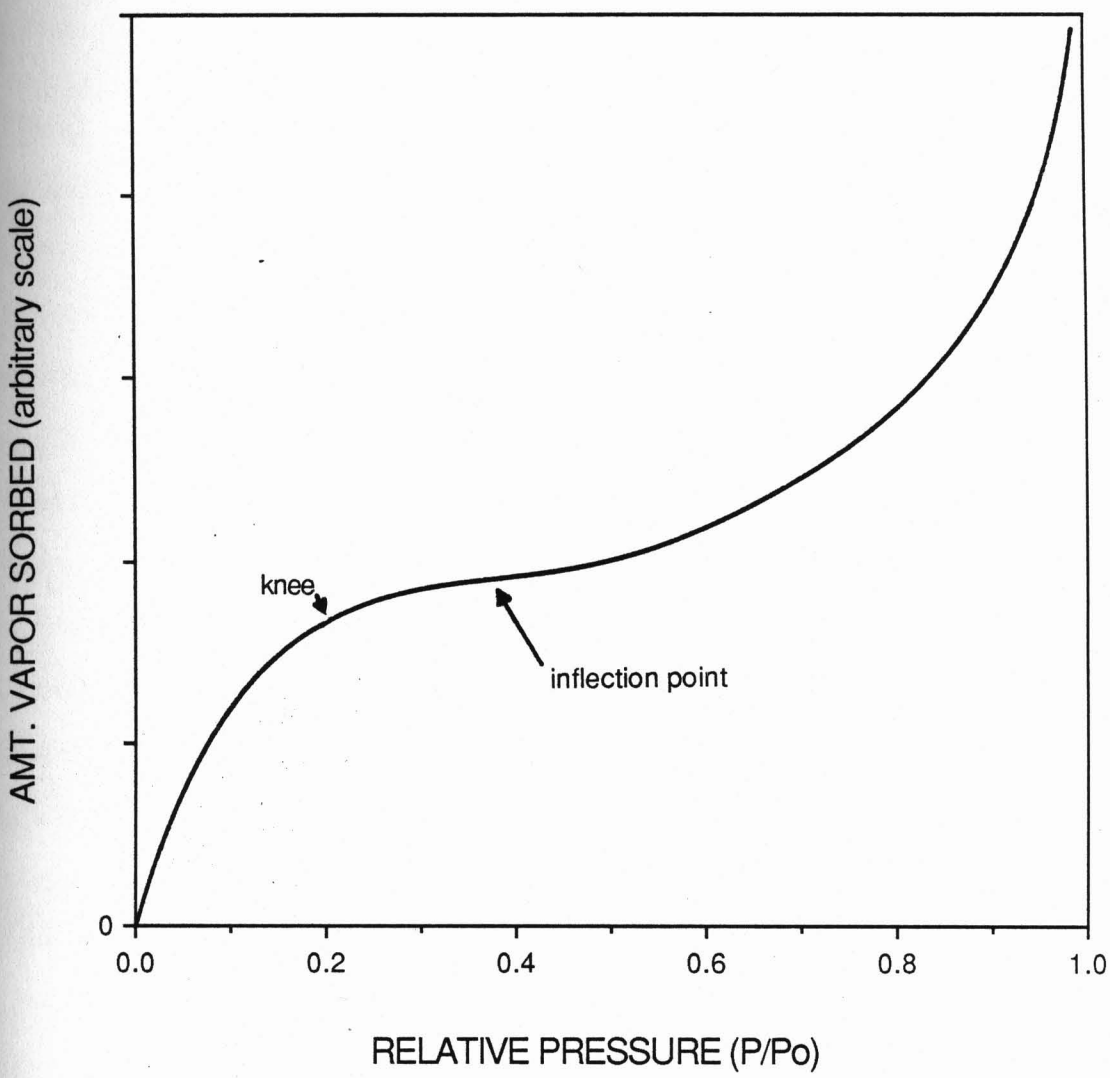

Figure 1: Vapor sorption isotherm.

through the linear portion of the isotherm, new vapor molecules adsorb onto molecules of the monolayer resulting in multilayer coverage.

The adsorption process is commonly separated into two general classes: physical adsorption and chemical adsorption (sometimes referred to as physisorption and chemisorption, respectively). Physical adsorption is considered to be the result of non-specific intermolecular interactions such as van der Waals forces or London dispersion forces between a gas molecule and a solid surface. It generally occurs at temperatures near the boiling point of the adsorbate. Its effects are usually fully reversible (i.e., the adsorbate may be removed by lowering the pressure or raising the temperature without affecting the adsorbent surface structure). Equilibrium usually occurs rapidly for physical adsorption since essentially no energy of activation is required. Chemical adsorption, as its name implies, suggests full chemical bonding characterized by large interaction potentials. Since a high chemical specificity exists between adsorbate and adsorbent molecules, the chemisorbed adsorbate is frequently difficult to remove. Desorption often leads to irreversible chemical changes.

Chemisorbed molecules are limited to a simple monolayer of coverage, whereas molecules physisorbed may occupy several layers. Both types of adsorption may occur simultaneously, with physical adsorption occurring on top of or along side of a chemisorbed layer. Further, it is possible for a molecule to rapidly adsorb in a physical manner, and then slowly enter into some chemical reaction with the solid surface. A more extensive and complete discussion of physical and chemical adsorption is presented by Adamson (23) and Lowell (24).

C. Vapor Adsorption Models

Many models describing vapor adsorption have been developed throughout the years. Langmuir (26) in 1918 proposed a classical model, based on the kinetic theory of gases, which accurately described vapor adsorption up to a single monolayer of coverage. The Langmuir equation may be expressed as:

$$W = \frac{W_m \ C_L \ (P/P_o)}{1 + C_L \ (P/P_o)} \qquad (1)$$

where W is the amount of vapor sorbed onto a solid (usually expressed as grams of vapor per gram of solid) at a

particular relative pressure, (P/P_o), W_m is the mass of vapor at monolayer coverage, and C_L is the Langmuir constant. Since chemisorption is restricted to monolayer coverage, it can often be described by the Langmuir equation. The multilayer coverage attainable in physical adsorption cannot, however, be completely described by the Langmuir theory.

In 1938, Brunauer, Emmett, and Teller (27) extended the work of Langmuir by developing a model (BET model) which accounted for vapor adsorption of more than one molecular layer in thickness. As in the Langmuir model, this model theorized that vapor molecules in the first molecular layer were tightly bound to identical sites of the adsorbent and that no interaction between sorbed molecules occurred. Beyond this first molecular layer, it was assumed that the second and higher layers reflected the characteristics of the bulk liquid phase. One form of the BET equation is written as follows:

$$W = \frac{W_m C_B (P/P_o)}{[1-(P/P_o)][1-(P/P_o)+C_B(P/P_o)]} \qquad (2)$$

where W, W_m and (P/P_o) are the same as for the Langmuir

equation and C_B is the BET constant expressed by:

$$C_B = k \exp[(H_1 - H_L) / RT] \quad (3)$$

where k is a constant related to the entropy of adsorption, but most often assumed to approximate unity. H_1 is the heat of adsorption of the first molecular layer, H_L is the heat of liquefaction or condensation of the molecule, R is the gas constant, and T is the absolute temperature. The BET equation can be rearranged to a linear form:

$$\frac{1}{W[(P_o/P)-1]} = \frac{1}{Wm\, C_B} + \frac{C_B - 1}{Wm\, C_B}(P/P_o) \quad (4)$$

so that the constants W_m and C_B can be calculated directly by the following expressions:

$$Wm = \frac{1}{\text{Slope} + \text{Intercept}} \quad (5)$$

$$C_B = 1 + \left(\frac{\text{Slope}}{\text{Intercept}}\right) \quad (6)$$

Experience with a wide range of vapors and solids (23,24,25) has shown that the BET model holds only over the relative pressure range $0.05 < P/P_o < 0.35$. This is partially so because the BET theory assumes that the second and higher layers of adsorbate are all equivalent to the liquid phase. Although this assumption may indeed be justified for molecules several layers away from the surface, its applicability may be somewhat questioned with layers closer to the surface.

Various modifications have been made by researchers to the BET model over the years which promote a better fit to adsorption data over the entire range of relative pressures. Caurie (28), Venkateswaren (29), and van den Berg and Bruin (30) have presented reviews of several models which have been derived to better fit such data.

One such model, the so-called GAB model, which combines previous work by Guggenheim (31), Anderson (32), and deBoer (33), was proposed by van den Berg (34) for describing water vapor sorption by various starches. The GAB model extends the BET model and provides a more accurate description of adsorption data over a wider relative pressure range. The advantage of the GAB model is that it allows for a third thermodynamic state of adsorbed vapor

intermediate to that of the tightly bound monolayer and the bulk liquid. In this way there is no distinctive separation between the bound vapor and the bulk liquid, but instead a layer of vapor is included which is in an intermediate thermodynamic state. The GAB equation is written in the following form:

$$W = \frac{Wm\ Cg\ K\ (P/P_o)}{[1-K(P/P_o)][1-K(P/P_o)+CgK(P/P_o)]} \qquad (7)$$

where W, W_m, and (P/P_o) are described in the previous sorption theories, and C_g and K are constants associated with the heats of the three thermodynamic states of adsorbate. C_g and K are given by the equations:

$$C_g = k' \exp[(H_1 - H_m) / RT] \qquad (8)$$

$$K = k'' \exp[(H_L - H_m) / RT] \qquad (9)$$

where H_1, H_L, R, and T have also been described previously, k' and k'' are constants, and H_m is the heat of adsorption of the intermediate vapor layer.

D. Water Vapor Sorption

Let us now consider water vapor as the specific adsorbate molecule. For many solids, the water vapor uptake isotherm exhibits a typical sigmoidal shaped curve when the equilibrium amount of sorbed water vapor is plotted as a function of thermodynamic water activity, a_w. Since we assume that ideal gas conditions exist at the temperatures under study, a_w can be approximated by the relationship:

$$a_w = P/P_o \qquad (10)$$

where P is the water vapor pressure in the system and P_o is the vapor pressure of pure water at the experimental temperature. Hence, the equilibrium uptake of water vapor is often reported as a function of one of the following:

1) water vapor pressure, P;

2) relative water vapor pressure, P/P_o;

3) relative humidity, $100(P/P_o)$; or

4) thermodynamic water activity, a_w.

It should be noted that for water-insoluble solids, as the water vapor pressure in the system is progressively increased, the isotherm generally asymptotically approaches

a water activity of one. For water-soluble solids, however, the isotherm will asymptotically approach a value equal to an equilibrium water vapor pressure equivalent to RH_o (i.e., that pressure above a saturated solution of the solid, the point of deliquescence).

Corn starch and microcrystalline cellulose are two common excipients utilized extensively in pharmaceutical systems and are components of primary focus in the present research. For these reasons, the interactions between water and these excipients deserve closer examination. Zografi and Kontny (6) presented a general model for water uptake on starches and celluloses in which they described the existence of at least three thermodynamic states of water. At low relative pressures, water is bound directly to available anhydroglucose units throughout the starch grain and in the amorphous regions of cellulose with a stoichiometry of one water molecule per anhydroglucose unit. At intermediate relative pressures, polymer-polymer hydrogen bonds can break providing an increase in primary binding sites available. This allows water to bind to other water molecules already bound to anhydroglucose units. Finally at even higher relative pressures, water can now also bind to other water molecules, including those not bound to primary

sites. The authors further provide evidence to show that the intermediate state or states of water exist out to about three times the value of W_m. This water is not directly bound to the primary site, yet it is still influenced by the chemical structure of the anhydroglucose unit.

Since the sorption of water vapor generally involves intermolecular forces on the order of that of hydrogen bonding, (rather than stronger chemical bonds), it can usually be described by one of the physical adsorption models described above. In work with a wide range of pharmaceutical excipients, Kontny (35,36) showed that water vapor sorption data adhered well to the GAB model in which the three thermodynamic states of water described above were assumed. Figure 2 shows a typical example for corn starch where the GAB model produced a more accurate representation of the sorption data than the BET model. Based on this work, as well as present studies ongoing in this laboratory, the GAB model will be used where applicable in the present work to describe the sorption of water vapor onto the pharmaceutical solids under study. It should be pointed out, however, that other multiparameter equations can also be used to fit such data. This is discussed in detail by Zografi and Kontny (6).

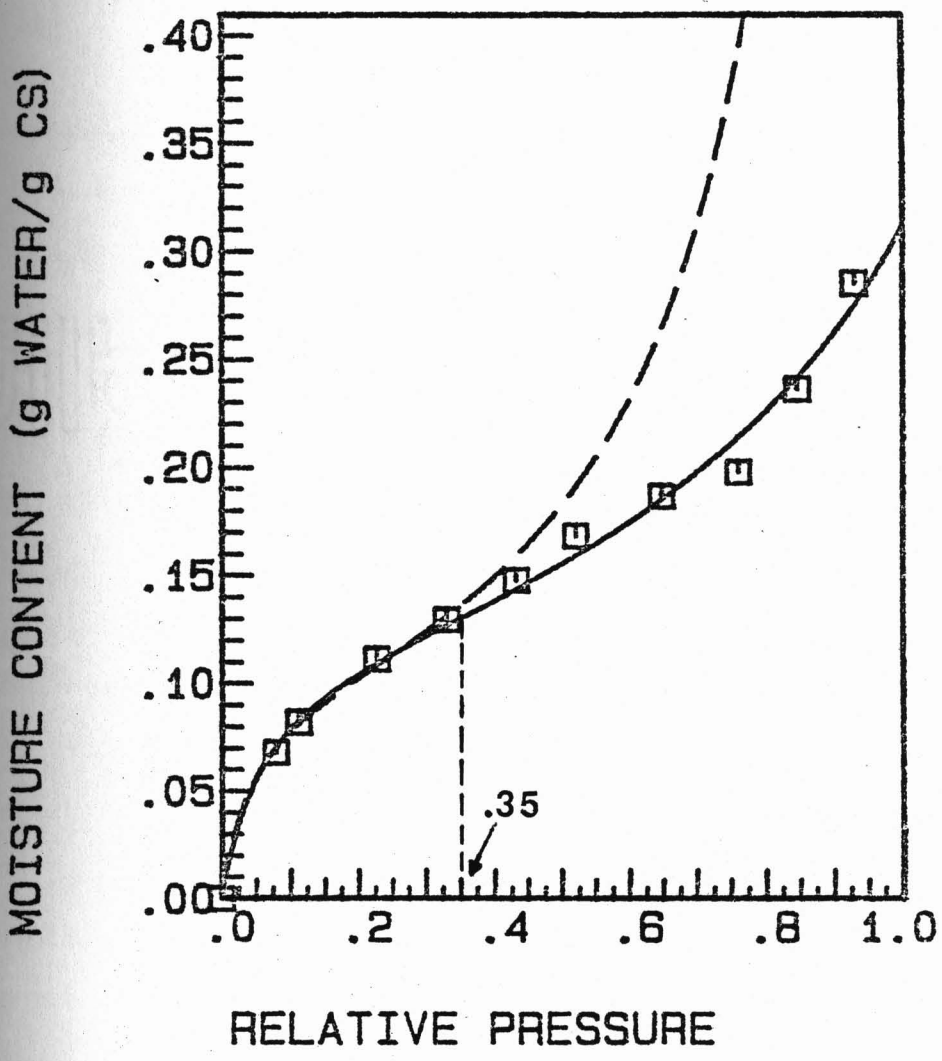

Figure 2: Fit of BET (-----) and GAB (———) equations to water vapor desorption data of corn starch at 20°C.
(Reprinted from reference 35.)

E. Hysteresis

A significant phenomenon which arises in vapor sorption studies is the hysteresis loop exhibited by many substances. As shown in Figure 3, the hysteresis loop is the region between the sorption isotherm (curve A) and the desorption isotherm (curve B). It is most commonly associated with porous solid adsorbents, however it is also seen for sorption into hydrophilic polymers. Lowell (24) described several shapes that the hysteresis loop may assume for porous systems and provided a brief explanation for these shapes based on the pore structure of the adsorbent. Van den Berg (34) described the hysteresis of polymers, such as cellulose and starch, as being due to conformational changes in the polymer chain when moisture enters the polymer structure. Bryan (37) used a thermodynamic approach in discussing the hysteresis effect in water-biopolymer systems. The presence of hysteresis yields an undesirable complication in that for a given relative pressure there are two distinct sorbed vapor concentrations possible, depending on the previous history of the system.

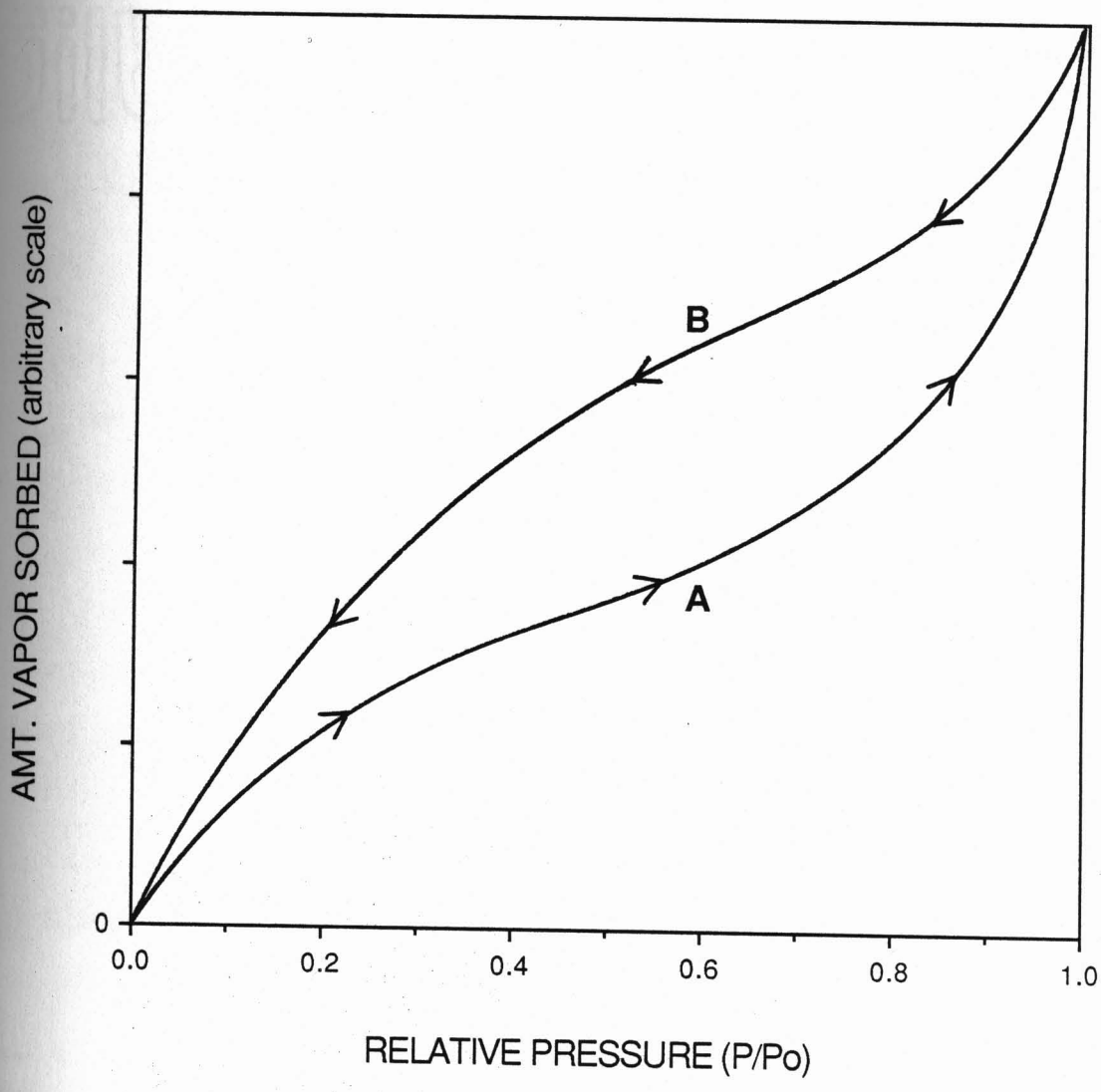

Figure 3: Sorption-desorption hysteresis.

F. Moisture Transfer

Let us now concern ourselves with the movement of water from one location to another during storage of a pharmaceutical product. First, consider the transfer of moisture between a closed product container and the outside environment. Moisture may enter or leave the container by one or both of the following mechanisms:

1) If the container is impermeable to water vapor (e.g., glass), then moisture enters or leaves only when the container is opened to the environment or by leakage through bottle caps.

2) If the container is permeable to water vapor (e.g., polymeric films), then moisture transfer may occur by diffusion through the film.

Moisture transfer always proceeds in a direction from high relative water vapor pressure to low relative water vapor pressure (i.e., moisture enters the system if the outside relative water vapor pressure is higher than the system, and moisture leaves the system if the outside relative water vapor pressure is lower than the system). Two extreme cases may be considered:

1) If the dosage form is composed primarily of hydrophobic components and the outside environment is

extremely dry (i.e., the relative water vapor pressure in the environment is significantly lower than within the container), a drying out of the dosage form resulting in brittleness would be expected.

2) If the dosage form is composed primarily of hydrophilic and/or hygroscopic components and the outside environment is extremely wet (i.e., the relative water vapor pressure in the environment is significantly higher than within the container), a considerable softening of the dosage form would be expected. Further, in the case of a drug which undergoes hydrolytic decomposition, these conditions would additionally potentiate chemical instability.

Water vapor transmission through product containers has long been recognized as a prevalent mechanism by which products become exposed to excess moisture. In 1958, Blaug, Hickman and Lach (38) studied the permeation of moisture through a variety of closures frequently employed to seal pharmaceutical containers. More recently, Peppas and Khanna (39,40) have examined the importance of water vapor diffusion through polymeric films commonly used as packaging materials for food systems. Several of the films considered are also used as pharmaceutical packaging materials. These

workers developed mathematical models which allow shelf-life predictions of food products based on the diffusion characteristics of the particular polymeric packaging film as well as the sorption characteristics of the food product. In a later publication (41), Peppas applied this work to pharmaceutical systems.

Another source of moisture which may affect the stability of pharmaceutical products is the moisture directly associated with the components of the formulation. It is desirable to know and understand whether or not a component which is introduced to a formulation with a high moisture content may have the ability to lose some of its moisture to a component which was originally introduced at a much lower moisture content. Two possible means for this moisture transfer exist:

1) via the vapor state, or

2) via diffusion of bulk liquid water.

Depending upon the specific storage conditions and the initial moisture contents of the various components, it is plausible that a combination of these two processes occurs simultaneously. The present study will focus and discuss in considerable detail moisture transfer solely via the vapor state in a closed system (i.e., the system has no

interaction with the outside environment) and the resulting establishment of thermodynamic equilibrium among all components.

A review of the literature produced several studies which examined moisture transfer among formulation components within a closed system. Strickland and Moss (42) studied the transfer of moisture between gelatin capsules and hygroscopic medicinals. After allowing each sample to equilibrate separately at desired relative humidities, pairs of samples were placed in closed containers. It was found that a moisture loss was exhibited by the sample initially equilibrated at the higher relative humidity and that moisture was correspondingly gained by the sample initially equilibrated at the lower relative humidity. Ito, Kaga, and Takeya (43) examined water vapor transfer between gelatin capsule-starch and gelatin capsule-microcrystalline cellulose combinations. The components were individually equilibrated over saturated salt solutions then placed in pairs in sealed glass containers. It was found that water transfer proceeded from the capsules to the powders, whose initial equilibrium relative humidities were lower than that of the capsules.

In a study using soft gelatin capsules (which may

contain 30-40% water), Serajuddin, Sheen, and Augustine (44) found that water migrated into the fill material. The fill material consisted of a poorly water soluble drug dissolved in polyethylene glycol 400. After 3 to 4 weks of storage, significant crystallization was observed and attributed to the migration of water into the fill material.

Bond, Lees, and Packington (45) demonstrated that moisture transfer was possible between gelatin capsules and a fill material consisting predominantly of cephalexin. Based on the sorption isotherm, it was necessary to maintain the capsules between 20-60% relative humidity. Below 20% the capsules became brittle and fractured, while above 60% the capsules softened. Examination of the cephalexin sorption isotherm showed that relative humidities of 20% and 60% corresponded to 5.7% and 7.5% moisture, respectively. Hence, to ensure acceptable physical characteristics of the capsule, these workers empirically chose the cephalexin to contain 5.7-7.5% moisture, thus minimizing deleterious moisture transfer effects.

Bell, Stevenson, and Taylor (46) studied moisture transfer between gelatin capsules and a fill material consisting of a sodium cromoglycate-lactose blend. These workers equilibrated both the capsules and powder blend at

identical relative humidities and found that this simple matching of equilibrium moisture activities did not eliminate moisture transfer effects. In fact moisture transfer occurred from capsules to powder. This effect was attributed to unusual hysteresis exhibited by the sodium cromoglycate. Sodium cromoglycate samples which had been successively cycled between 20% and 44% relative humidity showed consistent weight increases during each cycle rather than a return to original weight as would be expected in classical hysteresis. This finding was used to explain the moisture loss of the capsules and corresponding moisture gain by the powder blend. A similar finding was reported by York (47) in studies of gelatin capsules containing either maize starch-barbitone or maize starch-sodium barbitone powder blends. In each case a cycling of the filled gelatin capsules between 33% and 75% relative humidity showed a progressive loss in moisture from the gelatin capsules with the powder blends acting as a sink for it.

G. Previous Moisture Transfer Models

From the several examples presented in the previous section, it should be evident that moisture transfer among components may indeed play a prevalent role in instability

exhibited by pharmaceutical solids. It is desirable, therefore, to have the ability to predict *a priori* the final moisture activity of a product based upon initial activities of the individual components.

Ross (48), in studies with solutions, proposed a simple equation which related the final water activity, $(a_w)_f$, of a multicomponent solution to the individual activities of the separate components:

$$(a_w)_f = (a_w^o)_1(a_w^o)_2(a_w^o)_3 \ . \ . \ . \qquad (11)$$

This equation assumes that each component is dissolved in all of the water in the system and that each also behaves independently with respect to its water activity lowering ability.

Chirife (49) sought to apply the Ross equation to multicomponent mixtures of intermediate moisture foods which included water-insoluble materials. The insoluble materials tended to bind water and thus lowered water activity. In this case an "a_w^o" factor was assigned to each insoluble component assuming that all the water in the system was sorbed separately to each solid. This "a_w^o" factor was also reflective of the component's sorption isotherm. By

including the "a_w^o" factor for each insoluble component in equation 11, the author was able to reasonably predict the final moisture activity of various compositions of intermediate moisture foods. Due to the high water content of these intermediate moisture foods, however, the work was limited to the very high moisture activity region (a_w > 0.70). Many water soluble materials used in pharmaceutical products would be expected to undergo deliquescence in this high water activity region.

In a series of papers, Lang and Steinberg (50,51,52) derived a model for predicting water activity in multicomponent food systems. As a basis for the development of their model, these workers used a mass balance concept such that the final water content of the system was equal to the additive total of water provided by each individual component. This was described by the equation:

$$MW = \sum (m_i)(w_i) \qquad (12)$$

where M = moisture content of the mixture (g water/g solid), W = total dry weight of mixture, m_i = moisture content of

each component (g water/g solid), and w_i = dry weight of each component. Since m_i was unknown, Lang and Steinberg utilized the empirical Smith equation which relates m_i to water activity, a_w. The Smith equation can be expressed as:

$$m_i = b_i \log(1-a_w) + a_i \qquad (13)$$

where b_i = slope and a_i = intercept. Combining equations 12 and 13, the final equation for the working model was produced:

$$\log(1-a_w) = \frac{MW - \sum(a_i w_i)}{\sum(b_i w_i)} \qquad (14)$$

Lang and Steinberg showed good results for their model over the water activity range $0.30 < a_w < 0.95$ for binary and ternary mixtures of starch, casein, soy flour, salt, and sucrose. The model was limited, however, in that linearity of the Smith equation did not exist at water activities less than about 0.30.

Chuang and Toledo (53) derived an equation to predict the equilibrium moisture activity in binary mixtures of solids. Their approach was based on work by Norrish (54)

who measured the activity of binary sugar solutions. Chang and Toledo proposed the following equation to describe the water activity of a single component:

$$\log(a/N_1) = K(S_2)^2 + b \qquad (15)$$

where a = water activity, N_1 = moles water/100g solution, S_2 = g solute/100g solution, K = slope, and b = intercept. A plot of $\log(a/N_1)$ versus $(S_2)^2$ yielded multiphasic linear plots such that more than one slope (K) and intercept (b) existed for the same component. Using equation 15 for each individual component, a final equation which predicted moisture activity of binary mixtures was derived (the equation is not reproduced here due to its considerable length, but may be found in reference 53).

Although these authors showed reasonable agreement between predicted and experimental results for several starch-wheat mixtures, there are several problems in their approach. Firstly, for each component in the mixture, the range of initial to final equilibrium moisture activity must lie on the same line segment of the multiphasic linear plot of equation 15. This limitation restricts the ability to test materials over the entire range of moisture activity. Secondly, an assumption in their model requires the final

equilibrium water contents for each individual component to be equal. While this may have been a reasonable assumption in their work with starch and wheat, it can not be universally applied since, although equilibrium water activities are equal, equilibrium water contents necessarily are not. Finally, these workers did not allow for inclusion of the moisture present in the vapor state, which may be important in some cases.

In 1959 Salwin (55) and Salwin and Slawson (56) studied the effects of moisture transfer of dehydrated foods used as quick-serve meals by the Armed Forces. These workers developed a predictive model based on the moisture sorption isotherms of the individual components. Figure 4 depicts the moisture sorption isotherms for two arbitrary components, A and B. Components A and B have been stored at relative humidities of R_A and R_B, respectively, and have initial moisture contents of MA_1 and MB_1, respectively (expressed as per cent of dry solid). Salwin and Slawson proposed that if A and B are packaged together, then a transfer of water from B (higher relative humidity) to A (lower relative humidity) will occur until a final equilibrium relative humidity resulted, designated R_f. At

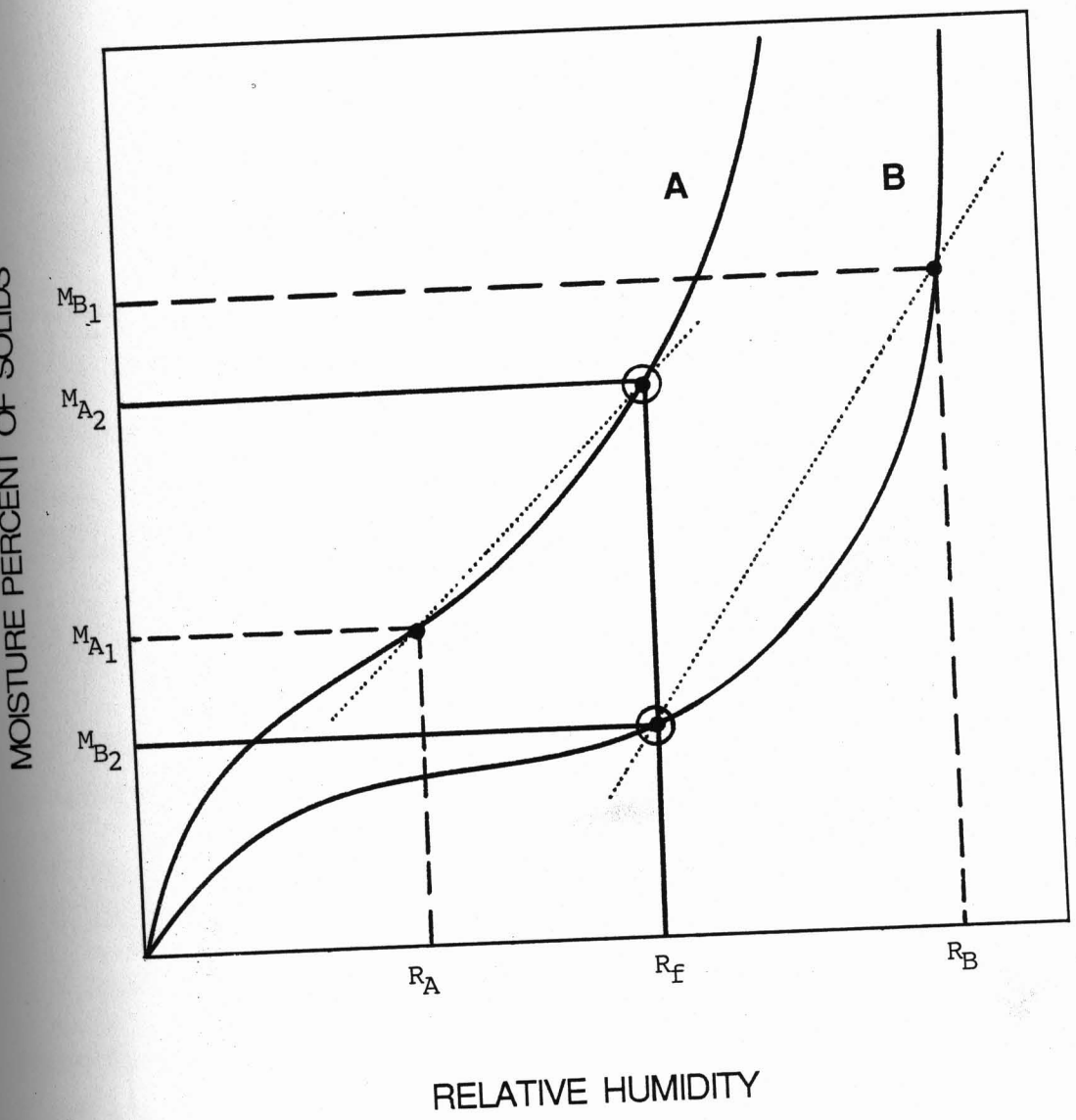

Figure 4: Salwin and Slawson's graphical representation of changes in moisture during equilibration.
(Reproduced from reference 55.)

this final relative humidity, components A and B will have new moisture contents M_{A_2} and M_{B_2}, respectively. Since the range of relative moisture activities (initial to final) is usually small for dehydrated foods, an assumption made in this model is that straight-line functions exist between initial and final relative humidities (shown as dotted lines in Figure 4). The slopes of these lines are given by:

$$S_A = \frac{M_{A_2} - M_{A_1}}{R_f - R_A} \qquad S_B = \frac{M_{B_2} - M_{B_1}}{R_f - R_B} \tag{16}$$

The weight gain of A is calculated by:

$$\text{Weight gain of A} = \frac{(M_{A_2} - M_{A_2})W_A}{100} = \frac{(R_f - R_A)S_A W_A}{100} \tag{17}$$

where W_A = dry weight of A. Similarly, the negative weight gain of B is:

$$\text{Weight gain of B} = \frac{(M_{B_2} - M_{B_1})W_B}{100} = \frac{(R_f - R_B)S_B W_B}{100} \tag{18}$$

where W_B = dry weight of B. In a closed system a mass balance of zero exists such that:

$$\text{Weight gain by A and B} = \frac{(R_f - R_A)S_A W_A}{100} + \frac{(R_f - R_B)S_B W_B}{100} = 0 \qquad (19)$$

Solving for R_f the following final equation results:

$$R_f = \frac{R_A S_A W_A + R_B S_B W_B}{S_A W_A + S_B W_B} \qquad (20)$$

W_A, W_B, R_A, and R_B are all parameters which are known or can be determined experimentally, and S_A and S_B are functions of R_f as given by equation 16.

Making a preliminary estimate of R_f allowed Salwin and Slawson to calculate the slope values, S_A and S_B. These values were then placed into equation 20 so as to obtain a better estimate of R_f. The new R_f value was then replaced back into equation 16. This iterative cycling between equations 16 and 20 was continued until the final equilibrium relative humidity was determined. Although this model was described for only two components, it could easily be extended to mixtures of several components.

These workers performed several experiments to verify the validity of this predictive model, all of which involved

the lower moisture activity range ($a_w < 0.37$). Their predicted results agreed closely with observed results in mixtures of up to 5 components of dehydrated foods.

The Salwin-Slawson approach is a useful one in that it utilizes the entire isotherm of each component, hence moisture transfer over the entire water activity range can be described. In its present form, however, several drawbacks exist when applied to the type of pharmaceutical components used in this study. First is the assumption of slope linearity between the initial and final relative humidities. Although this may be a valid assumption when moisture transfer occurs over a narrow range in the isotherm (as was the case in Salwin and Slawson's work), a high degree of error can result if the moisture transfer is over a wide range, where curvature in the isotherm exists. Second is the hysteresis exhibited by most compounds being investigated. Since at least one component involved in the moisture transfer must experience desorption, it is not entirely correct to use only the sorption branch of the isotherm as described by Salwin and Slawson. Lastly, account was not taken of the amount of moisture in the vapor state. For example, as indicated earlier, there are some situations where this could be important for many components

used in pharmaceutical systems which pick up only small amounts of water. In such cases the concentration of water in the vapor state may add a considerable effect to the results.

Ito, et. al. (43) applied the Salwin-Slawson model without modification to binary mixtures of gelatin-starch and gelatin-microcrystalline cellulose. Extrapolated initial relative humidities for each component were approximately: gelatin (64%), starch (24%), and microcrystalline cellulose (7%). Their predicted values of 44% for gelatin-starch and 41% for gelatin-microcrystalline cellulose were in reasonable agreement with experimental results.

II. STATEMENT OF THE PROBLEM

The following objectives and goals are necessary for completing this study:

1) To generate moisture sorption and desorption versus relative vapor pressure isotherms for all components to be examined (microcrystalline cellulose, corn starch, gelatin capsules and silica gel);

2) To measure the vapor pressure above physically separated individual components, then after allowing their head spaces to come in contact and equilibrate, measure the vapor pressure above the entire system; and

3) To develop a predictive model that allows the determination of the final moisture content in a mixture of components so long as certain initial characteristics of the individual components are known (e.g., weight, temperature, head-space volume and relative vapor pressure).

III. THEORY

A. The Sorption-Desorption Moisture Transfer (SDMT) Model

In the following theoretical discussion, moisture transport will be assumed to proceed solely via transmission through the vapor state. Consider a closed system in which two solid components, A and B, have been placed (as will be shown later, the proposed model can be extended to more than two components, though for simplicity only two will be considered at this time). The two components remain physically separated, though their head space volumes may or may not be allowed to interact. From Figure 5a, it is observed that when the two components are isolated from one another, a separate relative humidity, R_A or R_B, exists above each solid component in its respective head space volume, V_A or V_B. The precise relative humidity exhibited in each chamber is dependent on the total amount of water within the individual chamber, the amount of dry solid, and the binding affinity of the solid for water. In Figure 5b, the two chambers are now in contact allowing vapor to move freely from one to the other. A redistribution of moisture is expected resulting in a new final equilibrium relative

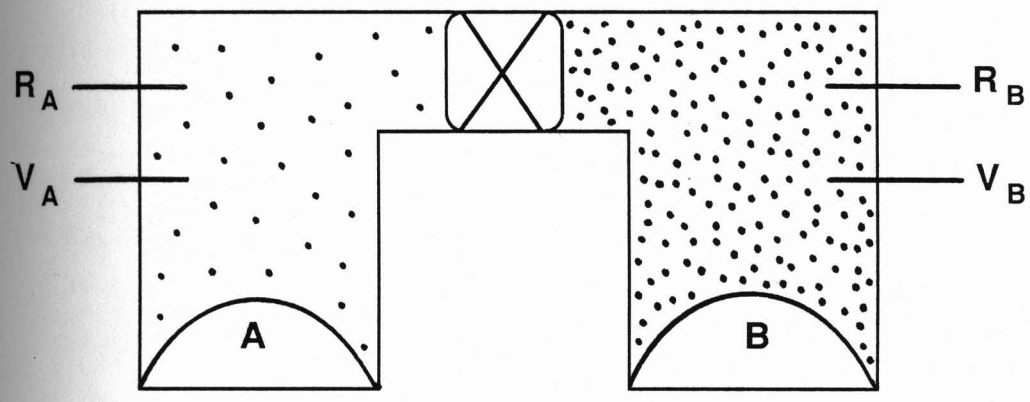

a) head spaces isolated from one another

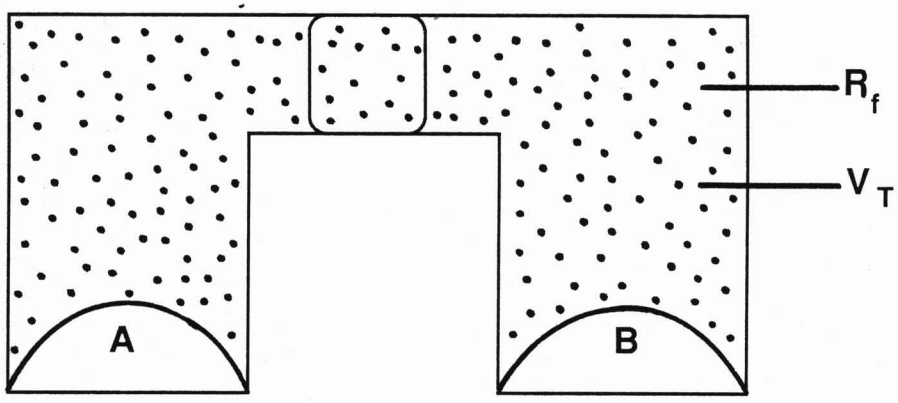

b) head spaces allowed to interact

Figure 5: Schematic for two component moisture transfer.

humidity, R_f, in the total head space volume, V_T. Not only will the moisture in the respective head space volumes redistribute, but moisture sorbed onto the solids will likewise redistribute depending on the relative affinity of water molecules, as well as the relative number of binding sites on the solids. Since initial conditions indicate $R_B > R_A$, it is likely that some of the molecules sorbed onto component B will desorb into the vapor space and subsequently sorb onto component A. This transfer of water molecules will continue until equilibrium is attained.

Figure 6 describes the same system using the moisture sorption isotherms for the two components, A and B, introduced into the system at relative humidities R_A and R_B, respectively. Using the isotherms for A and B the amounts of moisture associated with each can be determined as MA_1 and MB_1, respectively. Once the two components are exposed to one another, a redistribution of moisture occurs until a final equilibrium relative humidity, R_f, is established. R_f will be somewhere in between the two initial relative humidities, R_A and R_B. The moisture associated with A and B

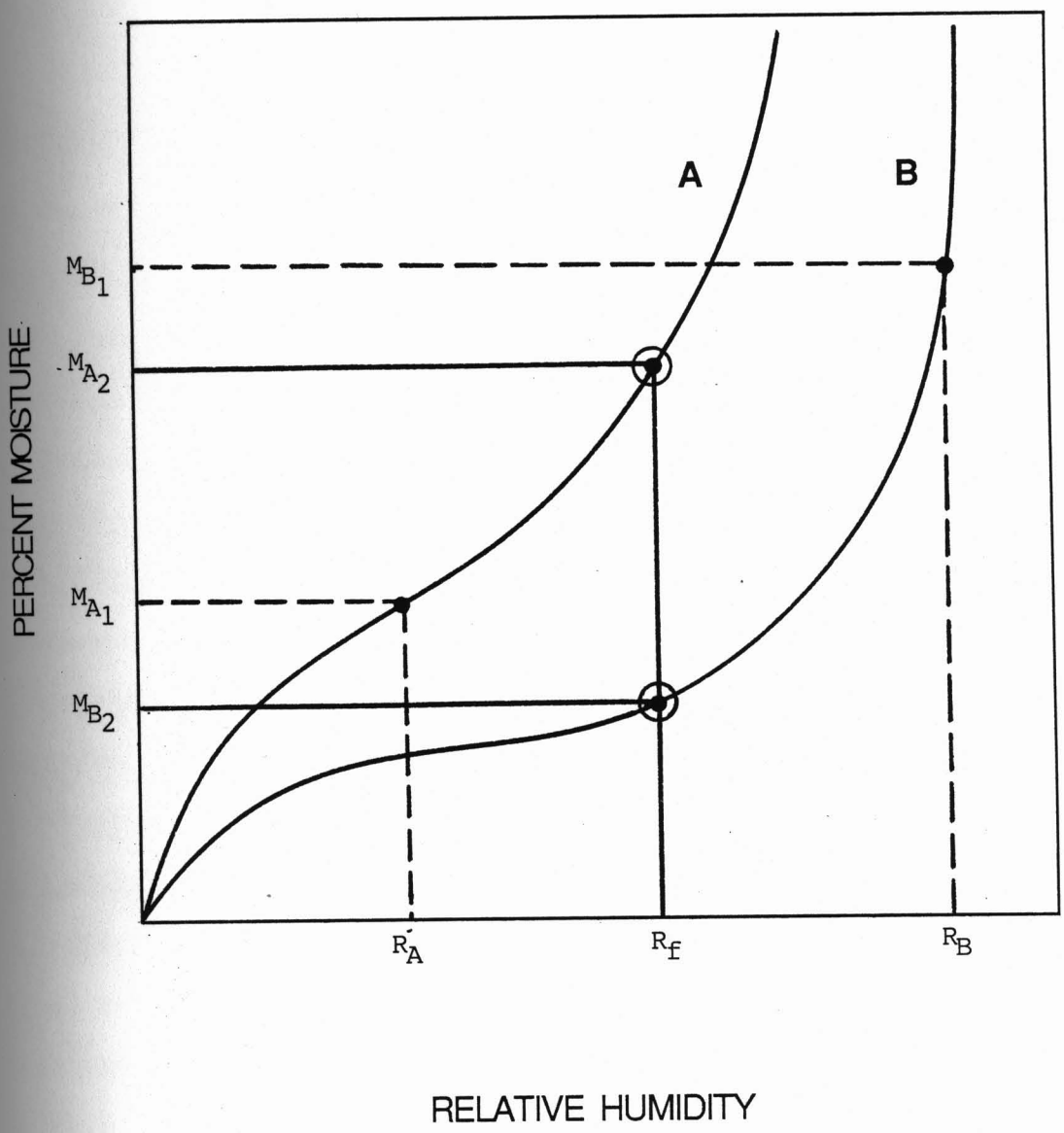

Figure 6: Sorption isotherms for two component moisture transfer.

at equilibrium can likewise be determined from the isotherms as MA_2 and MB_2, respectively.

Since the system is closed to the external environment, the total amount of moisture within the system remains constant, though moisture concentrations associated with the individual components will be subject to change until a thermodynamic equilibrium is established. It shoud be noted that a thermodynamic equilibrium does not imply each component will have an equal water content, but rather each component will exhibit the same activity of water (or relative water vapor pressure).

B. Modifications to the Salwin-Slawson Approach

The Salwin-Slawson (56) approach to predicting the final relative humidity above a mixture of components where moisture transfer is expected has been described previously in this thesis. The primary usefulness of this approach is that one is able to utilize the entire sorption isotherm for components under study, and hence, there are no limitations in the moisture activity range over which transfer can be evaluated. Although these workers obtained good results for mixtures of up to five components, most of their studies

were performed in the lower moisture activity range (a_w < 0.37).

Several drawbacks to the Salwin-Slawson model were also suggested previously, namely:

1) The assumption of slope linearity between initial and final relative humidities,

2) The neglect of any effect of hysteresis since only the sorption isotherm was considered, and

3) Moisture in the vapor state was not included.

Although the assumption of slope linearity may be valid when moisture transfer occurs over a narrow range in the isotherm, a high degree of error may result if the moisture transfer is over a wide range, especially where curvature in the isotherm exists. This potential error, however, can be minimized with the fit of sorption data to an equation describing the complete isotherm, such as the GAB equation.

Unless the desorption isotherm is identical to the sorption isotherm (i.e., no hysteresis), it is not entirely correct to use only the sorption branch of the isotherm. This is so because at least one component must experience desorption in the moisture transfer process.

Although the amount of moisture in the vapor state is probably negligible for mixtures where components have high

moisture contents, it may have a profound effect with components of very low moisture contents. For general applications, therefore, it is desirable to account for this vapor state moisture.

C. Derivation of the SDMT Model

Consider again two arbitrary components, A and B, as described by Figures 5 and 6. Initial moisture contents must first be determined. The total moisture in chamber A is the sum of the moisture associated with the solid component A and with the vapor state in the volume V_A. This can be described by the equation:

$$M_A = W_A GAB_A + IGL_A \tag{21}$$

where M_A = the total amount of moisture in chamber A, W_A = the dry weight of component A, GAB_A = the amount of moisture associated with component A as given by the GAB equation for A at its initial relative humidity R_A, and IGL_A = the amount of moisture in the head space volume, V_A, as given by the ideal gas law. When written out in its entirety, equation

21 takes the form:

$$M_A = W_A\left(\frac{Wm_A\, Cg_A\, K_A\, (P/P_o)_A}{[1-K_A(P/P_o)_A][1-K_A(P/P_o)_A+Cg_AK_A(P/P_o)_A]}\right) + \frac{P_oV_A(P/P_o)_A(18)}{RT} \qquad (22)$$

where W_m, C_g, and K have been described previously, $(P/P_o)_A$ $= R_A/100$ = the relative water vapor pressure, P_o = the pressure of pure water vapor at temperature T, and R = the gas constant. The second term on the right side of equation 22 has been multiplied by 18, the molecular weight of water, to obtain the amount of water vapor in grams. A similar equation can be written for the total amount of water in chamber B.

Once the total amounts of moisture have been determined for each individual chamber, the total moisture in the system, M_T, can be expressed by:

$$M_T = W_AGAB_A + W_BGAB_B + IGLv_T \qquad (23)$$

where the ideal gas law term is now written for the total head space volume, V_T, for the two chambers. Equation 23 written in its entirety takes the form:

$$M_T = W_A\left(\frac{Wm_A\, Cg_A\, K_A\, (P/P_o)}{[1-K_A(P/P_o)][1-K_A(P/P_o)+Cg_AK_A(P/P_o)]}\right) \qquad (24)$$

$$+ W_B\left(\frac{Wm_B\, Cg_B\, K_B\, (P/P_o)}{[1-K_B(P/P_o)][1-K_B(P/P_o)+Cg_BK_B(P/P_o)]}\right) + \frac{P_oV_T(P/P_o)(18)}{RT}$$

where (P/P_o) is now the final relative water vapor pressure in the equilibrated system following exposure of the two chambers to one another. Rearranging equation 24 and setting (P/P_o), the relative water vapor pressure, equal to "x", a fifth root polynomial equation is obtained.

$$x^5 + C_1x^4 + C_2x^3 + C_3x^2 + C_4x - C_5 = 0 \qquad (25)$$

where C_1, C_2, C_3, C_4, and C_5 are constants. The constant terms, made up of parameters in equation 24, are given in Appendix 1 for the convenience of the reader.

To solve equation 25, the real root between $(P/P_o) = 0$ and $(P/P_o) = 1$ must be found. Newton's method and an iterative technique have been used.

Newton's method utilizes the equation:

$$x_{n+1} = x_n - [f(x_n) \;/\; f'(x_n)] \qquad (26)$$

where $f(x_n)$ is equation 25 and $f'(x_n)$ is the derivative of equation 25 given by:

$$5x^4 + 4C_1x^3 + 3C_2x^2 + 2C_3x + C_4 = 0 \qquad (27)$$

To use Newton's method, a reasonable estimate for x_1 in equation 26 must first be chosen. The point on the x-axis where the tangent line to the function f at x_1 crosses gives the next estimate, x_2, to be used in equation 26. The sequence of x_n values converges to the desired root of equation 25. A BASIC computer program for an Apple II computer has been written which calculates this root (Appendix 2). A further description of Newton's method is available in most Calculus texts.

Newton's method was applied to a two component system where the constant terms in equation 25 previously had been determined. It is not possible to conveniently use Newton's method when more than two components are used, since for each component added in the moisture transfer process, an increase of two additional roots result in equation 25.

Although it is mathematically possible to determine the constant values for a higher order system, the computation involved makes this method somewhat impractical.

An iterative technique, therefore, was used to circumvent the necessity of converting equation 24 into the classical polynomial notation as given by equation 25. Since M_T remains constant in a closed system, an estimate for the relative water vapor pressure, $(P/P_o)_{est}$, in equation 24 can be used to determine M_T^{calc}, a calculated total moisture content in the system if the relative water vapor pressure equals $(P/P_o)_{est}$. If $M_T^{calc} > M_T$, then a lower estimate must be chosen for $(P/P_o)_{est}$. If $M_T^{calc} < M_T$, then a higher estimate must be chosen for $(P/P_o)_{est}$. If $M_T^{calc} = M_T$, then $(P/P_o)_{est}$ is the predicted final relative water vapor pressure in the system following moisture transfer.

A detailed description of the iterative technique using an n-component system will now be presented. Figure 7 provides a flow chart for this description. It is known that the final relative water vapor pressure must lie within

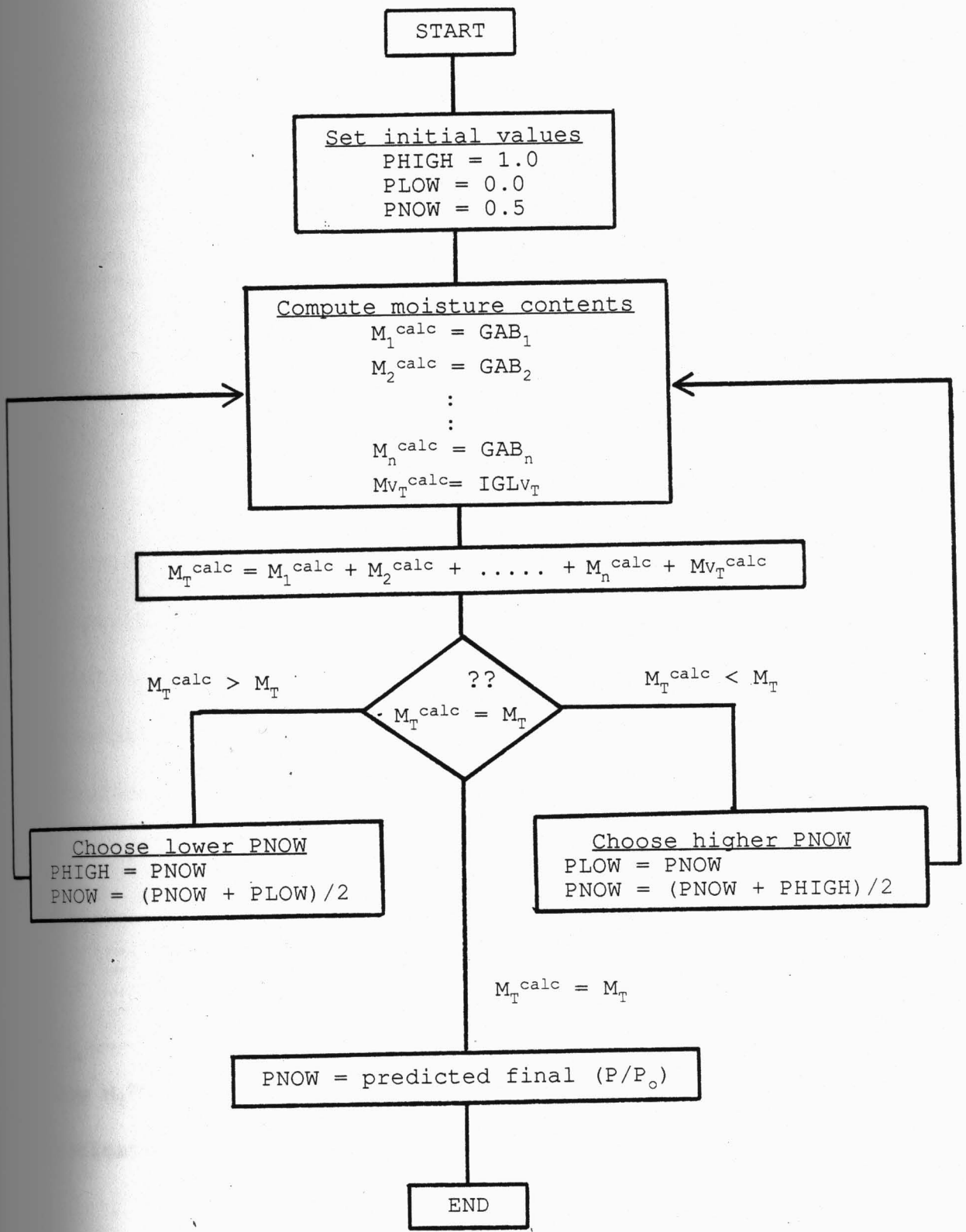

Figure 7: Flow chart for computer calculation of final relative water vapor pressure.

the range $0 < (P/P_o) < 1$. Hence, high and low relative pressure limits are given initial values (PHIGH = 1.0 and PLOW = 0.0). PNOW is the relative pressure estimate, $(P/P_o)_{est}$, being used to calculate M_T^{calc}. PNOW is given an initial estimate in the middle of the (P/P_o) range (i.e., PNOW = 0.5). Using this value of PNOW, the moisture content associated with each component in the system is computed using its respective GAB equation to give M_i^{calc} values, and the moisture content in the total vapor head space is computed using the ideal gas law to give MV_T^{calc}. The GAB constants used should appropriately reflect the sorption or desorption mode for the individual components. M_T^{calc} is obtained by summing the moisture contents of the individual components and the vapor state:

$$M_T^{calc} = \left(\sum M_i^{calc}\right) + MV_T^{calc} \qquad (28)$$

Now M_T^{calc} and M_T are compared. If $M_T^{calc} > M_T$, then a lower estimate is chosen midway between the present values of PLOW

and PNOW. If $M_T^{calc} < M_T$, then a higher estimate is chosen midway between the present values of PHIGH and PNOW. This process of choosing higher or lower estimates of PNOW proceeds until the desired root has been converged upon. When $M_T^{calc} = M_T$, the present value of PNOW becomes the predicted final relative water vapor pressure in the system. A BASIC computer program for the Apple II computer which performs this iterative technique is available in Appendix 3.

IV. EXPERIMENTAL

A. Materials

The following solids were used as sample components for experimental determinations of moisture transfer: microcrystalline cellulose[2], corn starch[3], gelatin capsules[4], and silica gel[5]. All components were stored under ambient conditions.

Table 1 provides a list of water soluble salts which were used in saturated solutions to produce various relative humidities. The relative humidities indicated are average values taken from several literature sources at 25°C.

B. Equipment

A schematic representation of the glass rack used for moisture transfer and sorption experiments is given in Figures 8a and 8b. The apparatus provides working vacuum pressures in the range of 10^{-5} to 10^{-7} torr. Apiezon[6] vacuum grease was used for all detachable ground glass

---

[2] Avicel PH101, FMC Corporation
[3] Argo, Best Foods
[4] Size no. 3, Eli Lilly Company
[5] 6-12 mesh, Fisher Scientific Company
[6] Type N, Apiezon Products Limited

Table 1

Relative Humidities of Saturated Salt Solutions at 25°C

Saturated Salt Solution	%RH	Reference
Phosphorous Pentoxide[7]	~0	---
Lithium Chloride[8]	11.6	57-64
Potassium Acetate[9]	21.5	57,58,60,61
Magnesium Chloride[7]	32.8	57-64
Potassium Carbonate[10]	43.2	57,58,60-62
Magnesium Nitrate[11]	53.2	57,58,60,61,64
Sodium Nitrite[12]	63.1	59,60,62
Sodium Chloride[7]	75.5	57-61,64,65
Potassium Bromide[13]	80.5	59,64
Potassium Chloride[10]	84.4	57-60,64-66
Potassium Nitrate[12]	93.1	57-61,63,64,66
Potassium Dichromate[14]	98.0	59,60

[7] Columbus Chemical Industries, Inc.
[8] Fisher Scientific Company
[9] Amend Drug and Chemical Company
[10] J.T. Baker Chemical Comapny
[11] MCB Manufacturing Chemists, Inc.
[12] Mallinckrodt Chemical Works
[13] Allied Chemical
[14] Mallinckrodt, Inc.

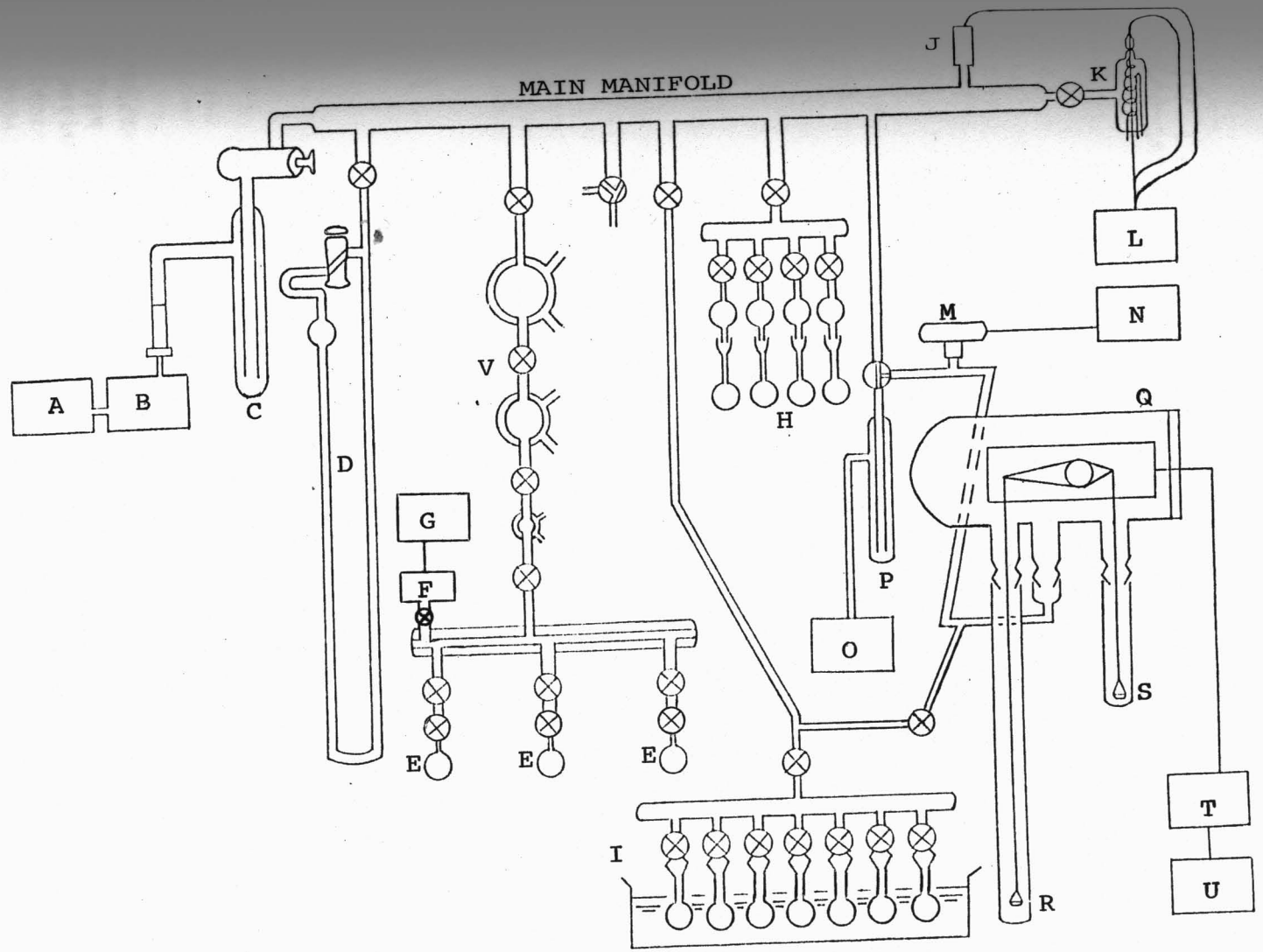

Figure 8a: Schematic of Moisture Transfer and Sorption Apparatus
Portions of this diagram were reproduced from reference 35.
⊗ denotes location of stopcocks

Figure 8b

Components of the Moisture Transfer and Sorption Apparatus

A. Vacuum pump #1[15]
B. Oil diffusion pump[16]
C. Liquid nitrogen cold trap
D. Oil manometer
E. Moisture transfer sample cells
F. Barocel pressure sensor[17]
G. Electronic manometer[18]
H. Relative humidity chambers
I. Relative humidity chambers
J. Pirani-type thermo gauge[19]
K. Ionization gauge[20]
L. Ionization gauge controller[21]
M. Pirani-type convection gauge[22]
N. Convection gauge controller[23]
O. Vacuum pump #2[24]
P. Liquid nitrogen cold trap
Q. Electrobalance[25]
R. Gravimetric sample pan
S. Gravimetric tare weights
T. Electrobalance control unit[25]
U. Chart recorder[26]
V. Moisture transfer compartments

---

[15] Model 1400, Sargent-Welch Scientific Company
[16] Type VMF-10, CVC Products, Inc.
[17] Type 600, Datametrics, Dresser Industries, Inc.
[18] Type 1400, Datametrics, Dresser Industries, Inc.
[19] Model 260009, Granville Phillips Company
[20] Model 274002, Granville Phillips Company
[21] Series 260, Granville Phillips Company
[22] Type 275, Granville Phillips Company
[23] Series 275, Granville Phillips Company
[24] Cenco Hyvac 7, Central Scientific Company
[25] Model RG-2002, Cahn Instruments, Division of Ventron Corporation
[26] Model 901, Altex Scientific, Inc.

fittings connected to the rack apparatus[27]. The apparatus was designed so that moisture transfer experiments and sorption experiments could be performed simultaneously.

Individual components of the rack include:

1. Vacuum pumps. Vacuum pump #1 was a mechanical backing pump for the oil diffusion pump. Vacuum pump #2 was used as a roughing pump to reduce the pressure in the system to less than 0.5 torr prior to using the diffusion pump.

2. Oil diffusion pump. The stainless steel diffusion pump was filled with silicone oil[28] and was capable of producing an ultimate vacuum pressure of about 10^{-8} torr. The oil was heated with a hot plate and the vertical pump stack was water cooled.

3. Oil manometer. A glass manometer was filled with silicone oil and used to measure the water vapor pressure of the saturated salt solutions.

---

[27] Note: To facilitate the flow of grease when connections were made, the grease was first softened by heating with a hand-held heat gun to a temperature of about 65°C.

[28] Type 704, Dow Corning Corporation

4. Moisture transfer sample cells. 50 milliliter round bottom Pyrex glass flasks with 14/20 ground glass fittings were used to house samples for moisture transfer experiments. The design of the sample cell, which allowed detachment of the cell while under vacuum, will be discussed in greater detail in the Methodology section. Each flask was immersed in a constant temperature water bath contained in a water-jacketed vessel. Mercury thermometers, with 0.1°C increments, were placed into each of these water-jacketed vessels to monitor actual sample temperature.

5. Barocel pressure sensor. This pressure transducer was connected directly to a small manifold which interconnected the three moisture transfer sample cell ports. It had a range of 100 torr, a sensitivity of 0.001 torr, and an accuracy of 0.15% of reading. Since the transducer was sensitive to room temperature fluctuations, it was enclosed by a water-jacketed vessel. Void space in the water-jacketed vessel was packed tightly with glass wool. The sensor was connected to an electronic digital manometer which displayed in units of torr. The primary purpose of this pressure sensor was to measure the water

vapor pressure during moisture transfer experiments.

6. Relative humidity chambers. Saturated salt solutions were used to provide various water vapor pressures. Double or triple distilled water was the solvent, and a sufficient quantity of salt was used such that excess solid remained undissolved. The saturated salt solutions were placed in round bottom Pyrex glass flasks with ground glass fittings and connected to the glass rack using Apiezon vacuum grease. To maintain constant temperature, the flasks were immersed in a temperature controlled water bath.

7. Pirani-type gauges. Two Pirani-type pressure transducers capable of pressure measurements from 10^{-3} to 1000 torr were mounted to the glass rack to monitor pressures in different areas. Each was connected to an analog output device. Due to the relative inaccuracy of the analog readout, these pressures were used strictly for reference purposes, and not in any subsequent calculations. Most importantly, these two pressure devices were used to detect the occurence of leaks and as an indication of when the pressure was sufficiently low to allow the use of the

oil diffusion pump.

8. Ionization gauge. The ionization gauge contained an iridium filament and provided pressure measurements from 2×10^{-10} to 10^{-3} torr. It was the only device capable of pressure measurement below 10^{-3} torr. The ionization gauge was connected to the ionization gauge controller which gave analog pressure readings.

9. Ionization gauge controller. This device was used for analog readouts of the ionization gauge and one of the Pirani-type pressure transducers.

10. Convection gauge controller. This device was used for analog readouts of one of the Pirani-type pressure transducers.

11. Electrobalance. The electrobalance components were contained in a vacuum belljar, and the sample pan and tare weight pan were suspended by fine stainless steel wire in hangdown tubes. The balance had a weight capacity of one gram. Sample weights were monitored continuously on a single pen chart recorder[29]. The electrobalance control

unit provided adjustments for the mass range and recorder range as well as controls for initially calibrating the electrobalance.

12. Moisture transfer compartments. Figure 9 depicts the various compartments of the moisture transfer apparatus. The apparatus was capable of holding three sample cells. The volumes of these cells varied with the sample size and hence are reported on an individual basis. The other compartments, labeled V_1 through V_4, were used as head space volumes, to which the moisture transfer cells could be exposed. In a practical sense, this provided the ability to simulate various product container sizes.

C. Methodology

1. Determination of relative humidities. As given in Table 1, relative humidities of saturated salt solutions were available from several literature sources at 25°C. The oil manometer was previously calibrated (35) at 25°C based on these literature values, and a linear regression equation was obtained:

---

[29] Model 155/MM, Altex Scientific, Inc.

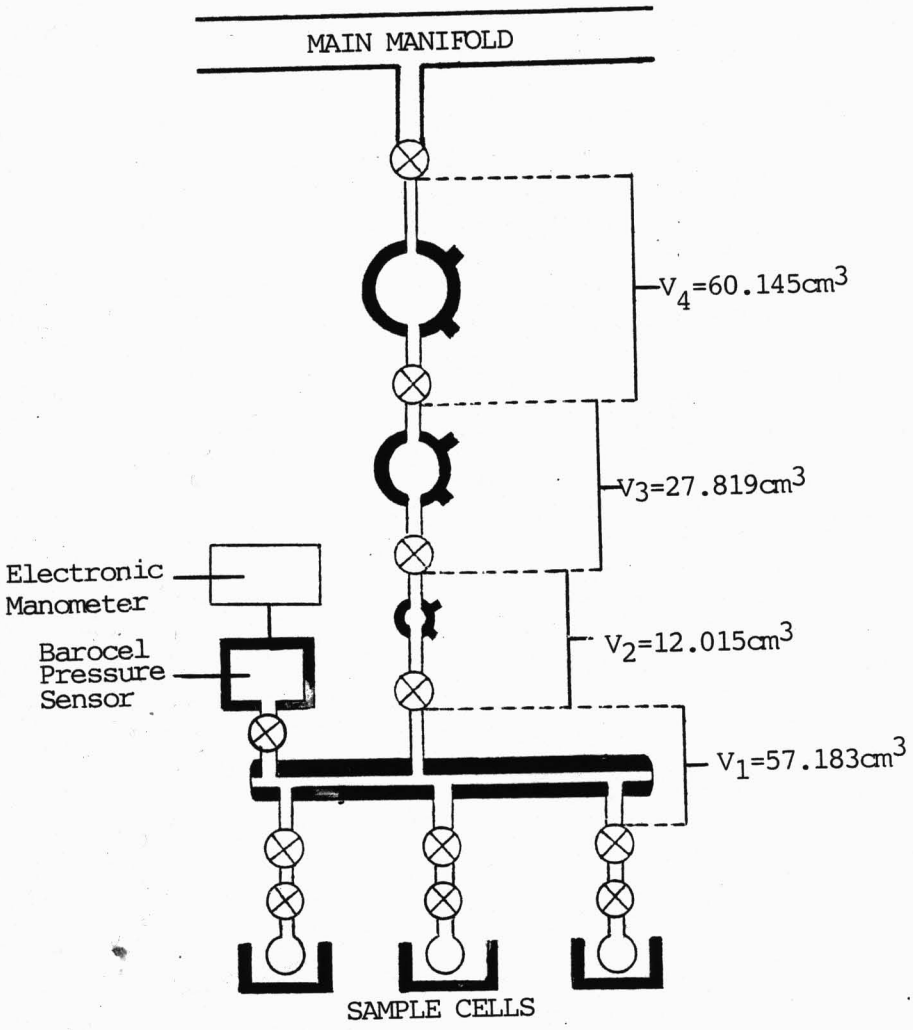

Figure 9: Moisture transfer compartments.
⊗ denotes stopcock locations
shaded areas indicate water-jacketed vessels

$$RH_{25} = (3.2926 \times P_{oil}) + 0.2522 \qquad (29)$$

where RH_{25} is the relative humidity at 25°C and P_{oil} is the equilibrium height difference between the two sides of the manomenter (in centimeters) when exposed to water vapor above a saturated salt solution.

Since the present work was performed at an experimental temperature of 23°C, it was necessary to adjust equation 29 so that relative humidities at 23°C could be determined. Assuming that water activity is independent of temperature, which is a reasonable assumption in this narrow temperature range, a simple conversion was made by multiplying equation 29 by the ratio of water vapor pressures of pure water at the calibration temperature to that at the experimental temperature:

$$\frac{(P_o)^{25}}{(P_o)^{23}} = \frac{23.756}{21.068} = 1.128 \qquad (30)$$

and,

$$RH_{23} = (3.713 \times P_{oil}) + 0.284 \qquad (31)$$

Table 2 lists the relative humidities at 23°C of the saturated salt solutions calculated from equation 31.

Each time a relative humidity chamber was opened and exposed to a sample or the oil manometer, its head space volume was purged at least three times to assure an environment of pure water vapor. This procedure was performed as follows:

a) isolate the sample from the system;

b) evacuate the main manifold;

c) open the desired relative humidity chamber and allow it to expand into the evacuated main manifold volume;

d) close off the relative humidity chamber; and

e) repeat steps b through d at least twice.

2. Desiccator moisture isotherms. A series of ten Pyrex glass desiccators were prepared with saturated salt solutions which provided the following relative humidities at 23°C: ~0, 11.3, 23.9, 34.1, 43.0, 54.6, 64.9, 75.2, 81.7, and 99.4 (all values in per cent). Desiccators and covers were sealed with Apiezon type N grease. Samples were placed into glass weighing bottles and weighed using a Mettler AC100 analytical balance[30] with a sensitivity of 0.0001

[30] Mettler Instrument Corporation

Table 2

Relative Humidities of Saturated Salt Solutions at 23°C

Saturated Salt Solution	P_{oil}	RH_{23}
Lithium Chloride	2.97	11.3
Potassium Acetate	6.35	23.9
Magnesium Chloride	9.12	34.1
Potassium Carbonate	11.50	43.0
Magnesium Nitrate	14.62	54.6
Sodium Nitrite	17.40	64.9
Sodium Chloride	20.18	75.2
Potassium Bromide	21.93	81.7
Potassium Chloride	22.67	84.4
Potassium Nitrate	24.93	92.9
Potassium Dichromate	26.70	99.4

grams. At approximately one week intervals, the samples were removed from their respective desiccators, reweighed, and immediately returned to the desiccator. Equilibrium was assumed when no more than about a 0.0050 gram weight change had occurred from the previous measurement. Once equilibrium was established, the samples were transferred to another relative humidity desiccator for a subsequent data point to be described in later subsections.

Since all moisture uptake values will be reported as grams of water per gram of dry solid, it was necessary to be able to calculate the dry weight of each sample. This was determined based on the weight loss of a sample placed over phosphorous pentoxide (~0% relative humidity). Samples of each component were placed in duplicate in a desiccator containing phosphorous pentoxide. After equilibrium was attained, the percent weight loss was calculated:

$$\text{percent weight loss} = [(W_i - W_f) / W_i] \times 100 \qquad (32)$$

where W_i and W_f are initial and final weights, respectively. An average percent weight loss was then determined from the duplicate samples. The dry weights of all other samples in

the study were calculated by subtracting this average percent weight loss from the initial net sample weights.

a. Sorption isotherms. Individual samples were placed separately into each of the ten relative humidity desiccators. Once equilibrium was attained, the amount of water per gram of dry solid was determined. These ten data points produced the moisture sorption isotherm.

b. Desorption isotherms. Nine samples were placed into the 99.4% relative humidity desiccator. When equiliibrium was established, the samples were removed and placed separately into each of the other lower relative humidity desiccators. Once equilibrium was attained, the amount of water per gram of dry solid was determined. These data produced the moisture desorption isotherm.

c. Desorption mini-isotherms. Samples used to obtain the sorption isotherms were also used for the desorption mini-isotherms. When a particular sample reached equilibrium, it was sequentially transferred to the next lower relative humidity desiccator. This provided desorption isotherms beginning at intermediate points along the main sorption isotherm.

d. Isotherm cycling. A sample of each component was sequentially cycled back and forth between 23.9 and 43.0%

relative humidity allowing equilibrium prior to each transfer.

3. Gravimetric moisture isotherms. Sorption and desorption isotherms were also obtained gravimetrically using the Cahn electrobalance. Sample weights were chosen on the basis of the water uptake characteristics of the solid and the experimental sensitivity desired. The balance was calibrated for each sample using class M high precision calibration weights[31]. Samples were placed on an aluminum sample pan then dried using heat (> 100°C) and high vacuum (< 10^{-3} torr). The dry weight was calculated directly from the chart recorder output and settings on the control unit. The samples were then sequentially exposed to a series of increasing relative humidities in increments of approximately 10 percent. Since the moisture uptake process was monitored continuously on the chart recorder, equilibrium was determined when no further weight increase was observed. Desorption isotherms were similarly obtained by sequentially exposing the samples to a series of decreasing relative humidities.

[31] Cahn Instruments, Division of Ventron Corporation

4. Computer fitting of isotherm data. Paramount to the predictive capabilities of the SDMT model was the ability to determine the quantity of water associated with a component at any given relative humidity. For microcrystalline cellulose, corn starch, and gelatin capsules this was achieved by applying the GAB equation (equation 7) to the sorption and desorption experimental data. Appendix 4 lists the Fortran computer program designed for a VAX/VMS computer which was used to accomplish this task. The program reads a data file which contains X,Y pairs corresponding to relative humidity and moisture uptake data, respectively. Using the GAB equation and a non-linear regression analysis subroutine, the program iterates to find the three parameters (W_m, C_g, and K) which provide the best mathematical fit to the experimental data.

Silica gel exhibited a hyperbolic curve which followed the Langmuir equation (equation 1). The Langmuir equation was rearranged to a linear plotting form:

$$\frac{(P/P_o)}{W} = \frac{1}{W_m C_L} + \frac{1}{W_m}(P/P_o) \qquad (33)$$

so that W_m and C_L could be obtained from the slope and

intercept, respectively. Once all constants were available, the moisture content associated with a component at any given relative humidity could be determined by application of the respective isotherm equation.

5. Moisture transfer.

a. Determination of sample dry weights. In order to perform these moisture transfer studies, it was necessary to dry the samples under vacuum conditions, then reweigh each sample without exposure to atmospheric conditions. Figure 10 depicts the sample cell assembly used for these experiments. The assembly consists of a sample cell and a sample cell holder which can be attached to the moisture transfer apparatus of the glass rack.

Samples were weighed directly into 50ml round bottom sample flasks on a Mettler H315 analytical balance[32] having a 1000 gram capacity and a 0.0001 gram sensitivity. An empty 150ml beaker was labeled as a "tare beaker" and used in all weighings to maintain the round bottom flasks in an upright position on the balance pan. The weight of the sample at this point was denoted "net weight before drying". Next, the sample cell was attached to the sample cell holder

[32] Mettler Instruments Corporation

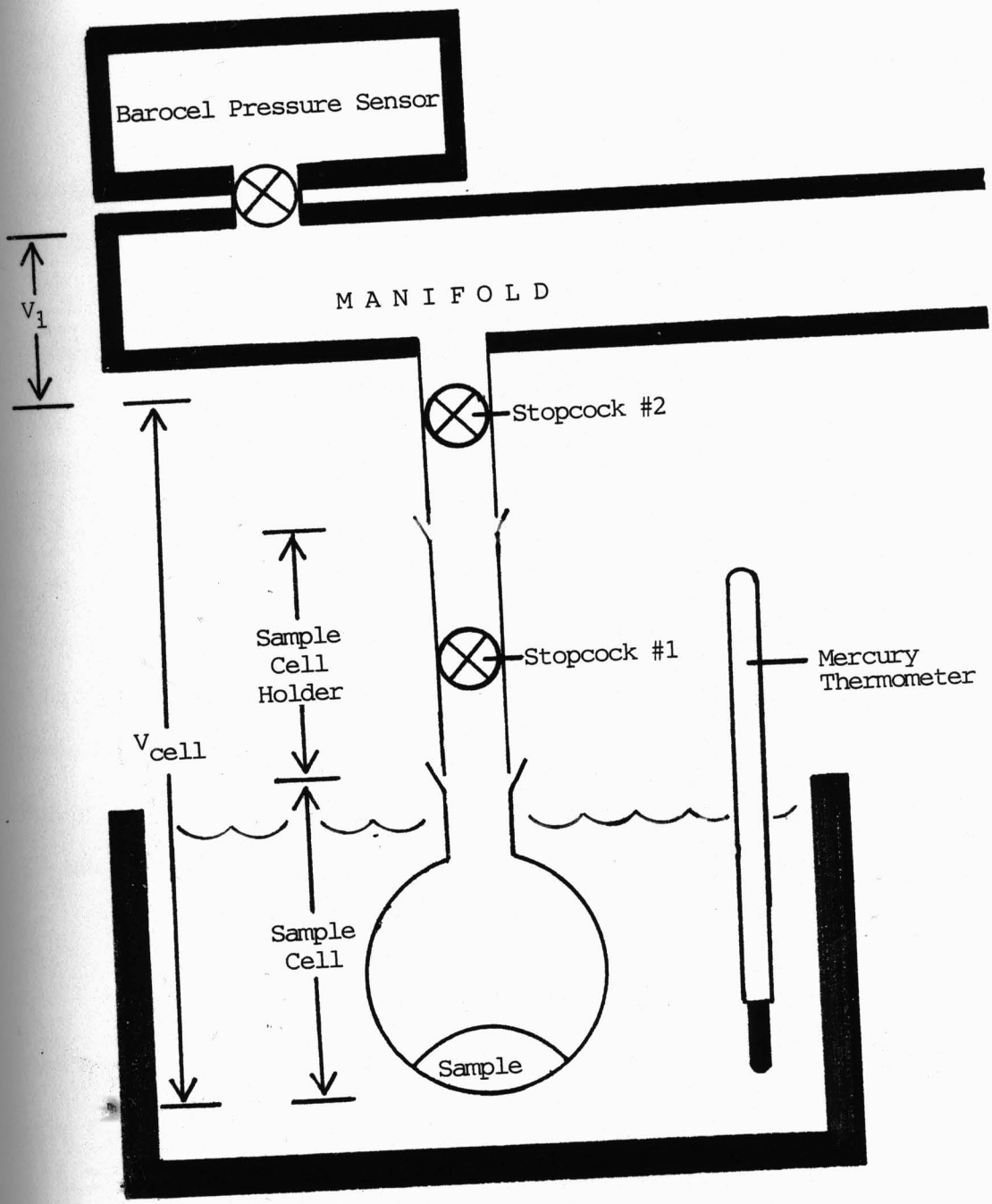

Figure 10: Design of the moisture transfer sample cell assembly.

⊗ denotes stopcock locations

shaded areas indicate water-jacketed vessels

and reweighed to obtain a gross weight of the assembly before drying. This assembly was then attached to the glass rack. With the moisture transfer apparatus under vacuum, the opening of stopcock #2 connected the sample cell holder to the glass rack, while opening of stopcock #1 connected the sample cell to the sample cell holder and began the drying process. Drying was facilitated by heating the sample to > 100°C with a heating mantle while under high vacuum. When drying was finished, stopcock #1 was closed to completely isolate the sample, then the assembly was detached from the glass rack and reweighed so as to obtain a gross weight of the assembly after drying[33]. The net weight loss was determined as:

$$\text{net weight loss} = W_{before} - W_{after} \tag{34}$$

where W_{before} is the gross weight before drying and W_{after} is the gross weight after drying. Finally, the sample dry weight was calculated as:

[33] Note: Residual grease remaining in the joint which connected the assembly to the glass rack was completely removed using toluene prior to reweighing.

dry weight = net wt before drying - net wt loss (35)

b. Determination of head space volumes. Head space volumes were determined using helium gas, assuming ideal gas conditions, and utilizing the relationship:

$$P_1V_1 = P_{total}V_{total} \quad (36)$$

where P and V denote pressure and volume, respectively, subscript "1" denotes compartment 1 of the moisture transfer apparatus, and subscript "total" denotes the sum of compartment 1 plus the sample assembly compartment. Since V_1 was known[34] and P_1 and P_{total} were measurable, V_{total} could be calculated. V_1 was filled with helium to a pressure between 30 to 40 torr. The pressure P_1 was measured directly using the Barocel pressure sensor. Stopcock #2 was then opened allowing the helium to expand into the sample cell assembly. This produced a new

[34] V_1 had been experimentally determined previously by first using a calibration cell which was filled with water. The volume of water was calculated by dividing the net weight of water by its density at the experimental temperature. With the calibration cell volume known, the volume of V_1 was determined by applying equation 36.

pressure, P_{total}, in the new volume, V_{total}. Since $V_{total} = V_1 + V_{cell}$, equation 36 can be rewritten:

$$P_1V_1 = P_{total} \times (V_1 + V_{cell}) \quad (37)$$

Solving for V_{cell}, the following equation results:

$$V_{cell} = (P_1V_1 / P_{total}) - V_1 \quad (38)$$

A minimum of three helium expansions were performed for each V_{cell} determination.

c. Moisture equilibration of samples. Samples were individually exposed to various relative humidities prior to beginning the moisture transfer process. Stopcocks #1 and #2 of the desired sample cell were opened, with all other sample cells closed, and exposed to a relative humidity chamber through the moisture transfer apparatus and the main manifold. Equilibration was allowed to occur overnight (longer times were necessary in some instances), and the pressure was measured directly using the Barocel pressure sensor. Stopcock #2 was then closed to isolate the sample

cell so that the other sample cells could be equilibrated in a similar manner.

d. Moisture transfer process. Once all sample cells were equilibrated to the desired relative humidities, stopcock #2 for each cell was opened allowing the head spaces of each cell to interact. Equilibration often required several days to occur, and the pressure was measured directly using the Barocel pressure sensor.

e. Calculation of relative humidities. Although the experimental temperature was controlled, slight deviations occurred as evidenced by the thermometers used to monitor sample temperatures. These deviations seldom exceeded $\pm 1^{\circ}C$ and were apparantly caused by room temperature fluctuations. An average temperture of the two or three sample cells in a given experiment, therefore, was determined. The vapor pressure of pure water, P_o, at this average temperature was used to calculate the experimental relative humidity as follows:

$$RH = (P/P_o) \times 100 \qquad (39)$$

where P is the measured experimental pressure.

f. Calculation of percent water. The percent of water associated with a particular solid component was obtained from the GAB equation for microcrystalline cellulose, corn starch, and gelatin capsules or the Langmuir equation for silica gel. Using the appropriate constants in the isotherm equation, the amount of water associated with one gram of the solid component could be attained at a given relative pressure. Multiplying the result by 100 yielded the percent water.

g. Calculation for the SDMT model. To proceed with this proposed model, equation 22 was first used to calculate the initial amount of water in each chamber. In this equation the GAB constants for the sorption branch of the isotherm were used since experimentally the components were thoroughly and fully dried before allowing initial moisture to equilibrate in the chamber. A total moisture content, M_T, in the system was then obtained by summing the initial moisture contents in the individual chambers. Since it was a closed system, M_T did not change. By placing this value of M_T into equation 24, then all terms were known except the final relative water vapor pressure, (P/P_o). It should be noted that in equation 24, since one of the components will

experience desorption, the GAB constants for the desorption branch of the isotherm were used for this component.

V. RESULTS AND DISCUSSION

Figures 11, 12, 13, and 14 provide moisture isotherms obtained gravimetrically for microcrystalline cellulose, corn starch, gelatin capsules, and silica gel, respectively. Figure 11 additionally provides the moisture isotherm obtained in desiccators for microcrystalline cellulose which yielded good agreement with the previous gravimetric data. Although the gravimetric isotherms for microcrystalline cellulose and corn starch were performed at 20°C, Kontny (35) showed that the moisture uptake of these components was independent of temperature over the range 20° to 50°C. Hence, for calculation purposes in the predictive model, GAB constants at 20°C were used for these two components when the experimental temperature was 23°C. Since previous isotherms were not available from this laboratory for gelatin capsules and silica gel, gravimetric moisture isotherms were obtained at the experimental temperature of 23°C. Only the sorption isotherm is presented for silica gel since its purpose in these studies was as a desiccant which only experiences the uptake of water.

Table 3a lists the GAB constants at various temperatures for microcrystalline cellulose, corn starch,

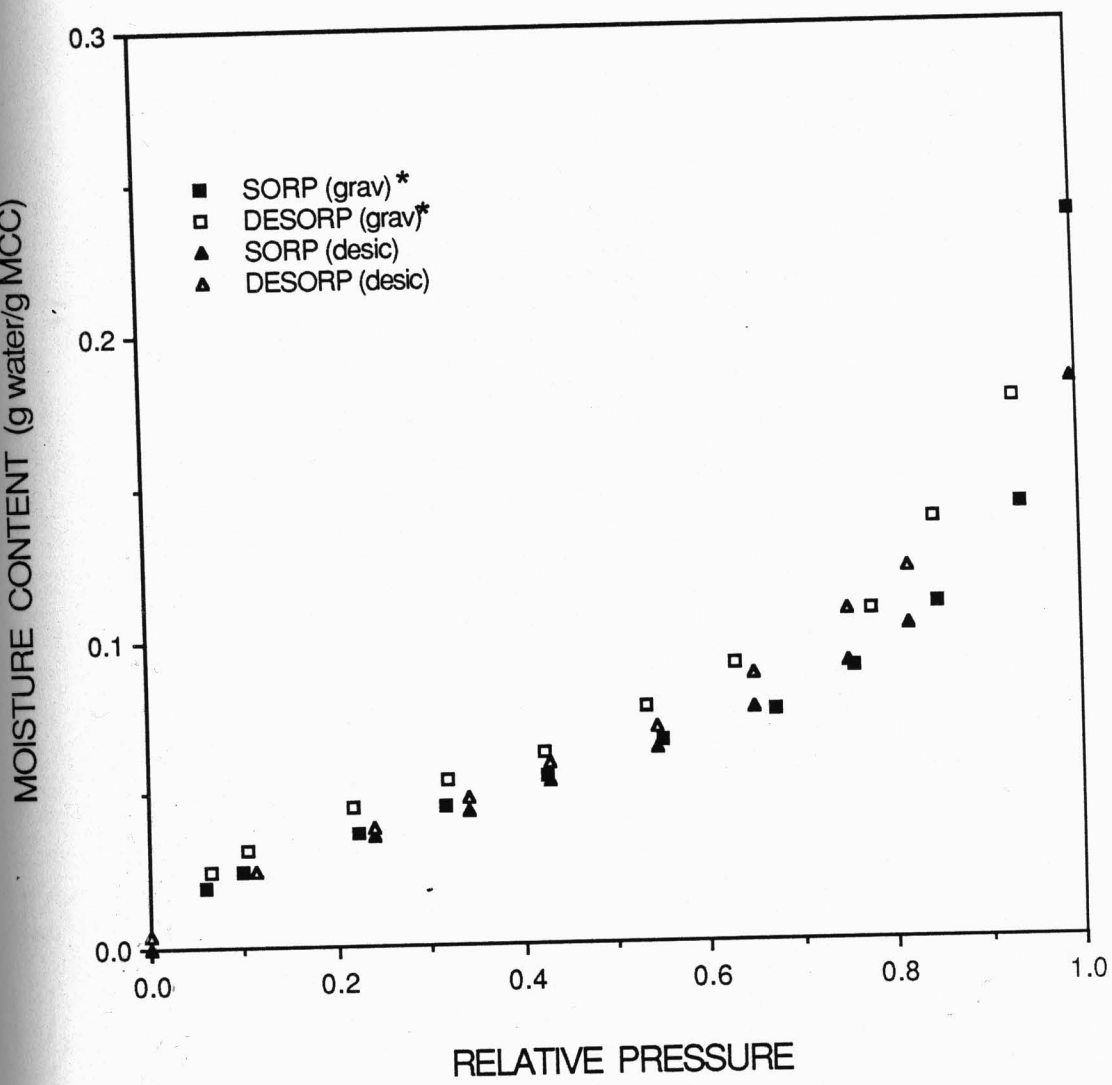

Figure 11: Sorption and desorption isotherms for microcrystalline cellulose.

Gravimetric, 20°C
Desiccator, 23°C

*Gravimetric data from reference 35.

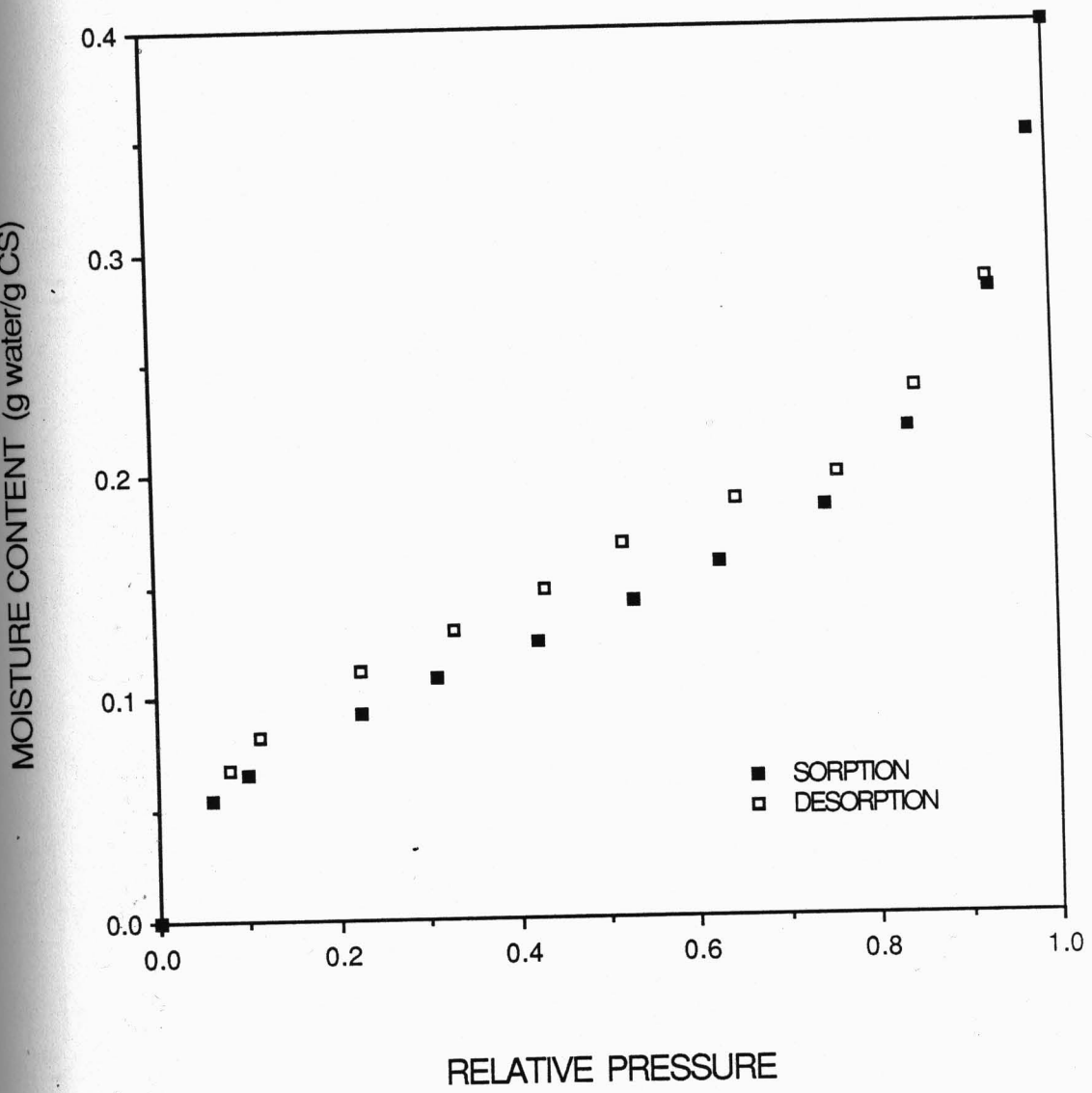

Figure 12: Sorption and desorption isotherms for corn starch.

Gravimetric, 20°C (data from reference 35).

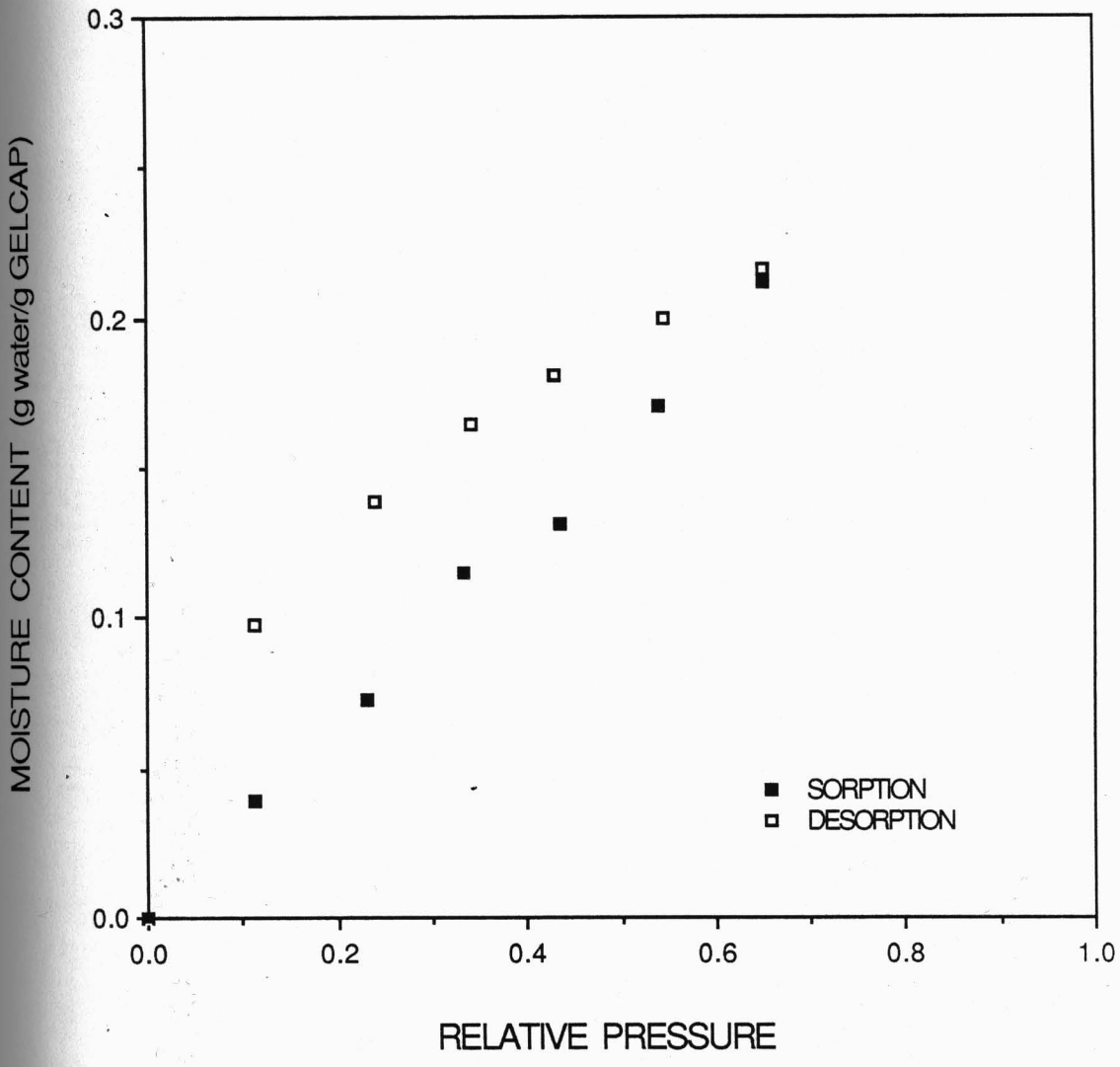

Figure 13: Sorption and desorption isotherms for gelatin capsules.

Gravimetric, 23°C

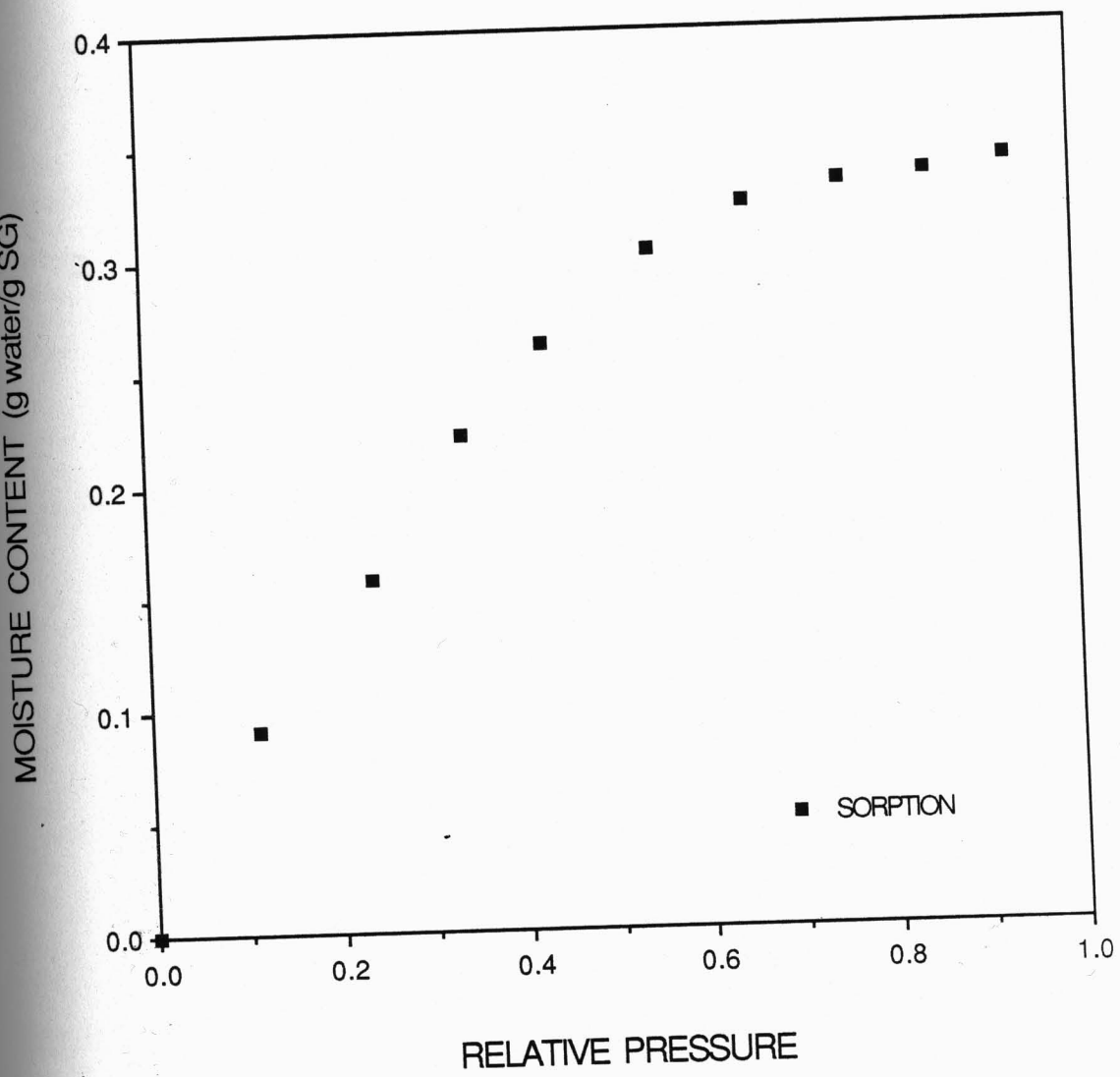

Figure 14: Sorption isotherm for silica gel. Gravimetric, 23°C.

Table 3a

GAB CONSTANTS

COMPONENT	MODE	TEMP (°C)	W_m‡	C_G	K
Microcrystalline cellulose*	Sorption	20	0.0299	55.7	0.870
	Desorption	20	0.0429	24.7	0.820
	Sorption	25	0.0285	49.5	0.893
	Desorption	25	0.0403	16.6	0.844
Corn starch*	Sorption	20	0.0753	67.0	0.804
	Desorption	20	0.114	26.9	0.641
Gelatin capsules+	Sorption	23	0.169	3.47	0.650
	Desorption	23	0.186	22.3	0.377

Table 3b

LANGMUIR CONSTANTS

COMPONENT	MODE	TEMP (°C)	W_m‡	C_L
Silica gel+	Sorption	23	0.572	1.78

‡ units = grams of water per gram of dry sample
*From reference 35
+From present work (gravimetric study)

and gelatin capsules. The Langmuir constants for silica gel are given in Table 3b.

Tables 4 through 9 give predicted versus experimental results for various binary combinations of microcrystalline cellulose, corn starch, and gelatin capsules. The initial dry weights and experimental temperatures are also given. Since the pressure in the system was the actual measurable quantity, results are given as percent relative humidity, $(P/P_o) \times 100$. Since the percent water gives a better indication of moisture actually associated with a particular solid component, it was also calculated based on both the predicted and experimental results. The GAB constants used for these calculations reflect sorption or desorption depending upon the mode the component was exhibiting during the transfer process. This is clearly seen in Table 4 where both sample cells contained microcrystalline cellulose. Although the percent relative humidity of the final mixture is the same for each sample, the percent water values differ since MCC-1 experienced sorption while MCC-2 experienced desorption during the transfer process.

Table 6 provides an additional column for the predicted results using the Salwin-Slawson approach (equations 16 and 20). The respective GAB equations for the sorption

Table 4

Predicted versus Experimental Moisture Transfer Results between Microcrystalline Cellulose and Microcrystalline Cellulose

INITIAL				FINAL			
MCC-1		MCC-2		% RH of FINAL MIXTURE		MCC-1 % H_2O based on	MCC-2 % H_2O based on
%RH	%H_2O	%RH	%H_2O	Predicted	Exp'l	Predicted Exp'l	Predicted Exp'l
10.6	2.6	50.3	5.0	28.2	31.6	3.6 3.8	4.4 4.7
31.6	3.8	65.1	6.7	46.6	49.2	4.7 5.0	6.1 6.4

Dry weights: Microcrystalline cellulose-1 = 3.3855g
Microcrystalline cellulose-2 = 5.2133g
Temperature: 25°C

Table 5

Predicted versus Experimental Moisture Transfer Results between Microcrystalline Cellulose and Corn Starch

INITIAL				FINAL					
MCC		Corn Starch		% RH of FINAL MIXTURE		MCC % H_2O based on		Corn Starch % H_2O based on	
%RH	%H_2O	%RH	%H_2O	Predicted	Exp'l	Predicted	Exp'l	Predicted	Exp'l
91.8	14.8	~0	~0	28.0	24.5	4.9	4.6	9.2	8.8
93.2	15.7	24.5	8.8	64.2	49.0	8.7	6.8	15.3	12.1
92.8	15.5	49.0	12.1	70.8	63.3	9.9	8.6	17.3	15.1
95.5	17.6	63.3	15.1	78.9	74.7	11.9	10.8	20.4	18.7
~0	~0	93.8	30.4	77.7	56.2	9.1	5.7	21.9	16.7
56.2	5.7	99.2	37.0	93.3	84.9	15.8	11.4	27.7	24.3

Dry weights: Microcrystalline cellulose = 4.9506g
Corn starch = 5.3209g
Temperature: 23°C

Table 6

Predicted versus Experimental Moisture Transfer Results between Microcrystalline Cellulose and Corn Starch

INITIAL				FINAL						
				% RH of FINAL MIXTURE			MCC % H_2O based on		Corn Starch % H_2O based on	
MCC %RH	MCC %H_2O	Corn Starch %RH	Corn Starch %H_2O	Predicted*	Predicted+	Exp'l	Predicted	Exp'l	Predicted	Exp'l
85.0	11.4	~0	~0	2.7	6.1	10.7	2.6	3.3	6.1	7.1
83.9	11.0	10.7	7.1	36.7	39.4	28.0	5.8	4.9	10.7	9.2
83.7	10.9	28.0	9.2	48.4	48.9	44.7	6.8	6.3	12.1	11.4
99.0	21.5	44.7	11.5	72.5	75.0	72.5	10.9	10.3	18.8	17.9
98.5	20.8	72.5	17.9	83.3	83.8	84.0	13.5	13.5	22.9	23.0
~0	~0	12.8	7.4	6.6	5.5	6.9	2.3	2.5	5.9	6.6
~0	~0	78.9	20.4	69.5	55.2	41.7	5.6	4.5	16.5	14.1
~0	~0	83.1	22.5	74.4	62.7	49.8	6.5	5.2	18.1	15.5
41.7	4.5	80.0	20.9	75.5	67.4	56.8	7.1	5.8	19.1	16.8
6.9	2.5	97.8	35.1	92.3	91.4	86.6	14.5	12.1	26.8	24.9

Dry weights: Microcrystalline cellulose = 5.0968g
Corn starch = 7.4013g
Temperature: 20°C

*Predicted using the Salwin-Slawson model.
+Predicted using the SDMT model.

Table 7

Predicted versus Experimental Moisture Transfer Results between Microcrystalline Cellulose and Corn Starch

INITIAL				FINAL					
MCC		Corn Starch		% RH of FINAL MIXTURE		MCC % H_2O based on		Corn Starch % H_2O based on	
%RH	%H_2O	%RH	%H_2O	Predicted	Exp'l	Predicted	Exp'l	Predicted	Exp'l
99.9	22.9	~0	~0	0.8	5.1	0.6	2.3	2.3	5.8
~0	~0	97.8	35.0	96.0	78.6	18.1	9.4	29.0	22.2
34.1	4.1	62.3	14.9	45.6	48.9	4.8	5.1	14.8	15.4

Dry weights: Microcrystalline cellulose = 1.5292g
Corn starch = 14.8028g
Temperature: 23°C

Table 8

Predicted versus Experimental Moisture Transfer Results between Microcrystalline Cellulose and Corn Starch

INITIAL				FINAL					
MCC		Corn Starch		% RH of FINAL MIXTURE		MCC % H_2O based on		Corn Starch % H_2O based on	
%RH	%H_2O	%RH	%H_2O	Predicted	Exp'l	Predicted	Exp'l	Predicted	Exp'l
96.0	18.1	~0	~0	88.3	38.7	15.3	5.8	25.8	10.6
38.7	4.4	61.2	14.6	40.0	46.3	4.4	4.9	13.8	14.9
72.7	8.1	32.3	10.0	56.6	63.4	7.6	8.6	13.6	15.1
~0	~0	95.2	31.9	8.6	25.8	2.6	3.6	7.4	11.5

Dry weights: Microcrystalline cellulose = 14.3760g
Corn starch = 1.5408g
Temperature: 23°C

Table 9

Predicted versus Experimental Moisture Transfer Results between Microcrystalline Cellulose and Gelatin Capsules

INITIAL				FINAL					
MCC		Gelatin Capsules		% RH of FINAL MIXTURE		MCC % H_2O based on		Gelatin Capsules % H_2O based on	
%RH	%H_2O	%RH	%H_2O	Predicted	Exp'l	Predicted	Exp'l	Predicted	Exp'l
95.1	17.2	~0	~0	74.8	72.1	10.8	10.2	25.2	24.0
~0	~0	72.1	24.0	16.1	15.3	3.1	3.1	11.7	11.4
53.0	5.4	80.2	27.9	66.3	63.8	7.0	6.6	21.9	21.5
~0	~0	99.7	41.5	54.0	34.7	5.5	4.1	19.9	16.5

Dry weights: Microcrystalline cellulose = 7.0041g
Gelatin capsules = 1.7848g
Temperature: 23°C

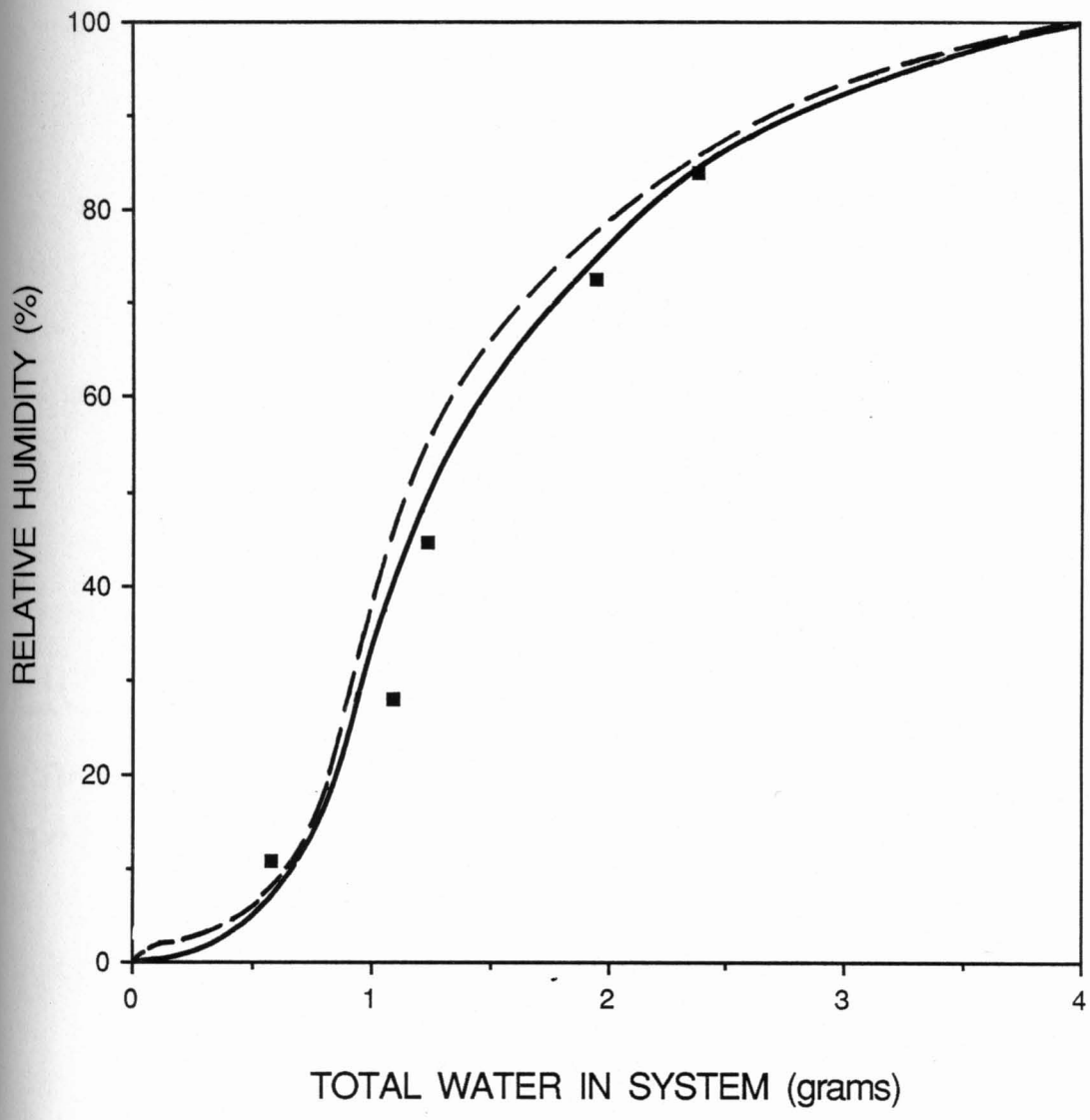

Figure 15: Moisture transfer between microcrystalline cellulose and corn starch where microcrystalline cellulose desorbs.

----- Salwin-Slawson prediction
——— SDMT model prediction

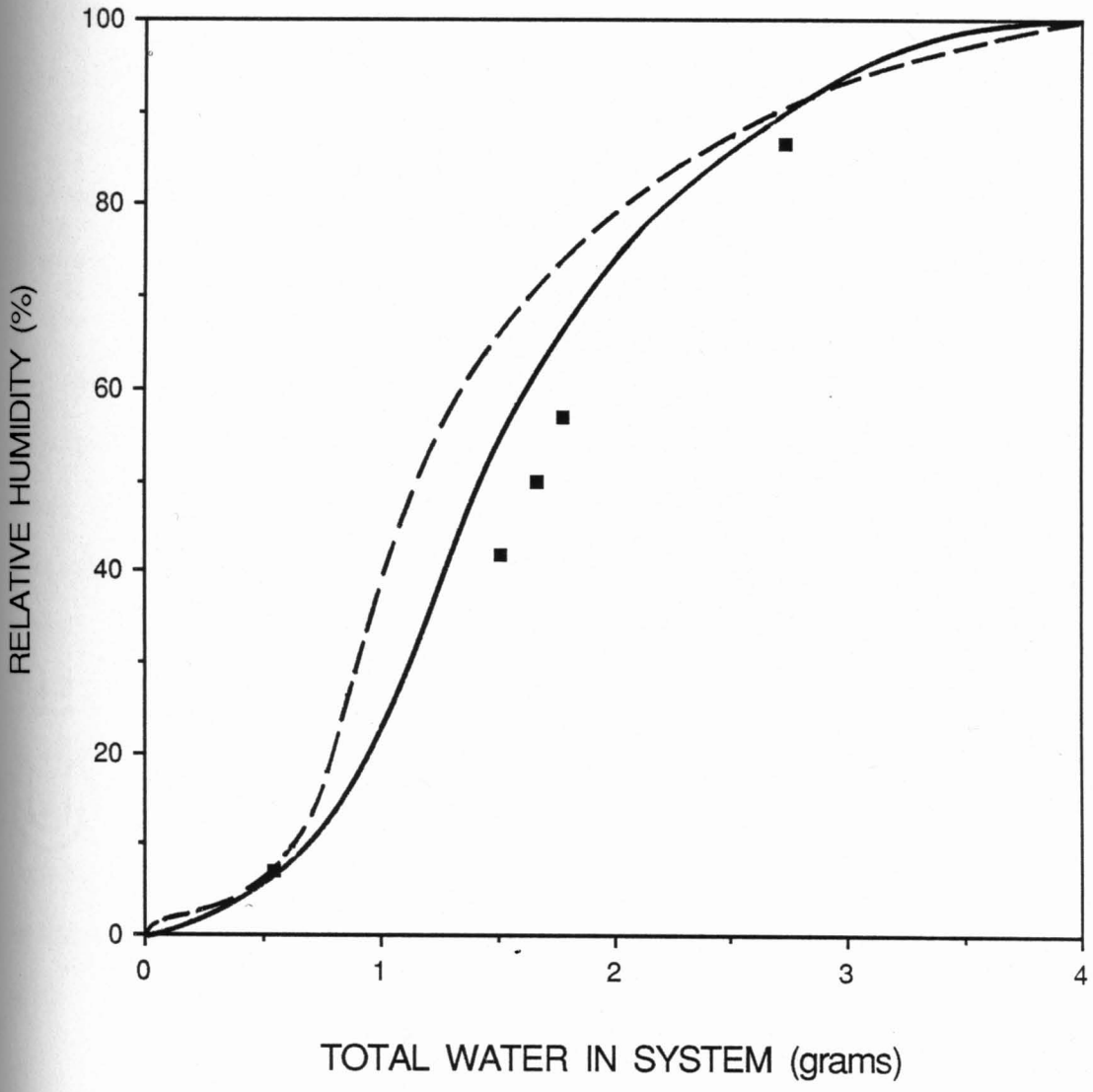

Figure 16: Moisture transfer between microcrystalline cellulose and corn starch where corn starch desorbs.

----- Salwin-Slawson prediction
——— SDMT model prediction

isotherms were used to calculate the moisture content values for equation 16. Figures 15 and 16 are graphical representations of the results given in Table 6 where the percent relative humidity is plotted as a function of total water in the system. Figure 15 presents results from the top five rows of Table 6 where microcrystalline cellulose desorbs in all transfers, and Figure 16 presents results from the bottom five rows of Table 6 where corn starch desorbs in all transfers. In Figure 15, the Salwin-Slawson model predicts slightly higher relative humidities than the SDMT model where the desorbing component, microcrystalline cellulose, exhibits relatively minimal hysteresis. In Figure 16, however, the deviation between the two models becomes greater since the desorbing component, corn starch, exhibits more significant hysteresis. Fit, in all cases with the SDMT model, appears as good and better.

Table 10 gives the predicted versus experimental results for a ternary mixture of microcrystalline cellulose, gelatin capsules, and silica gel. Since silica gel was found to follow the Langmuir equation, it was necessary to modify equation 24 to include this third solid component. A fourth term was added to the right side of equation 24:

$$W_C \left(\frac{W_{m_C} C_{L_C} (P/P_O)}{1 + C_{L_C}(P/P_O)} \right) \qquad (40)$$

Table 10

Predicted versus Experimental Moisture Transfer Results among Microcrystalline Cellulose, Gelatin Capsules and Silica Gel

INITIAL

MCC		Gelatin Caps		Silica Gel	
%RH	%H_2O	%RH	%H_2O	%RH	%H_2O
64.3	6.7	64.3	20.7	~0	~0
75.5	8.6	75.5	25.6	~0	~0
78.3	9.3	78.3	26.9	~0	~0
84.5	11.2	84.5	30.3	~0	~0

FINAL

% RH of FINAL MIXTURE		MCC %H2O based on		Gelatin Caps %H2O based on		Silica Gel %H2O based on	
Predicted	Exp'l	Predicted	Exp'l	Predicted	Exp'l	Predicted	Exp'l
20.5	24.8	4.3	4.6	13.1	14.3	15.3	17.6
31.6	31.5	5.2	5.2	15.9	15.8	20.6	20.6
35.5	41.2	5.5	6.0	16.6	17.7	22.2	24.2
47.0	41.8	6.6	6.1	18.7	17.8	26.1	24.4

Dry weights: Microcrystalline cellulose = 5.5200g
Gelatin capsules = 2.4698g
Silica Gel = 2.0934g
Temperature: 23°C

where W_c is the dry weight of silica gel and all other terms are described previously in the Langmuir theory.

The results obtained in these moisture transfer experiments have, in general, produced good results between experimental observations and SDMT model predictions. The present model is able to more accurately predict the final relative humidity when compared to the previous Salwin-Slawson approach.

Possible Sources of Error

Although many of the predicted results are in excellent agreement with the experimental observations, there are several instances where deviations occur. These deviations appear to be most prevalent when one component is initially equilibrated at a very high relative humidity, while the other is equilibrated at a very low relative humidity. It is suggested that two possible effects may account for these occurrences.

1. Error at very high and very low relative pressures. Figure 17 depicts the potential error that is possible at the extreme portions of an isotherm, where the change in amount sorbed with a change in relative pressure is great.

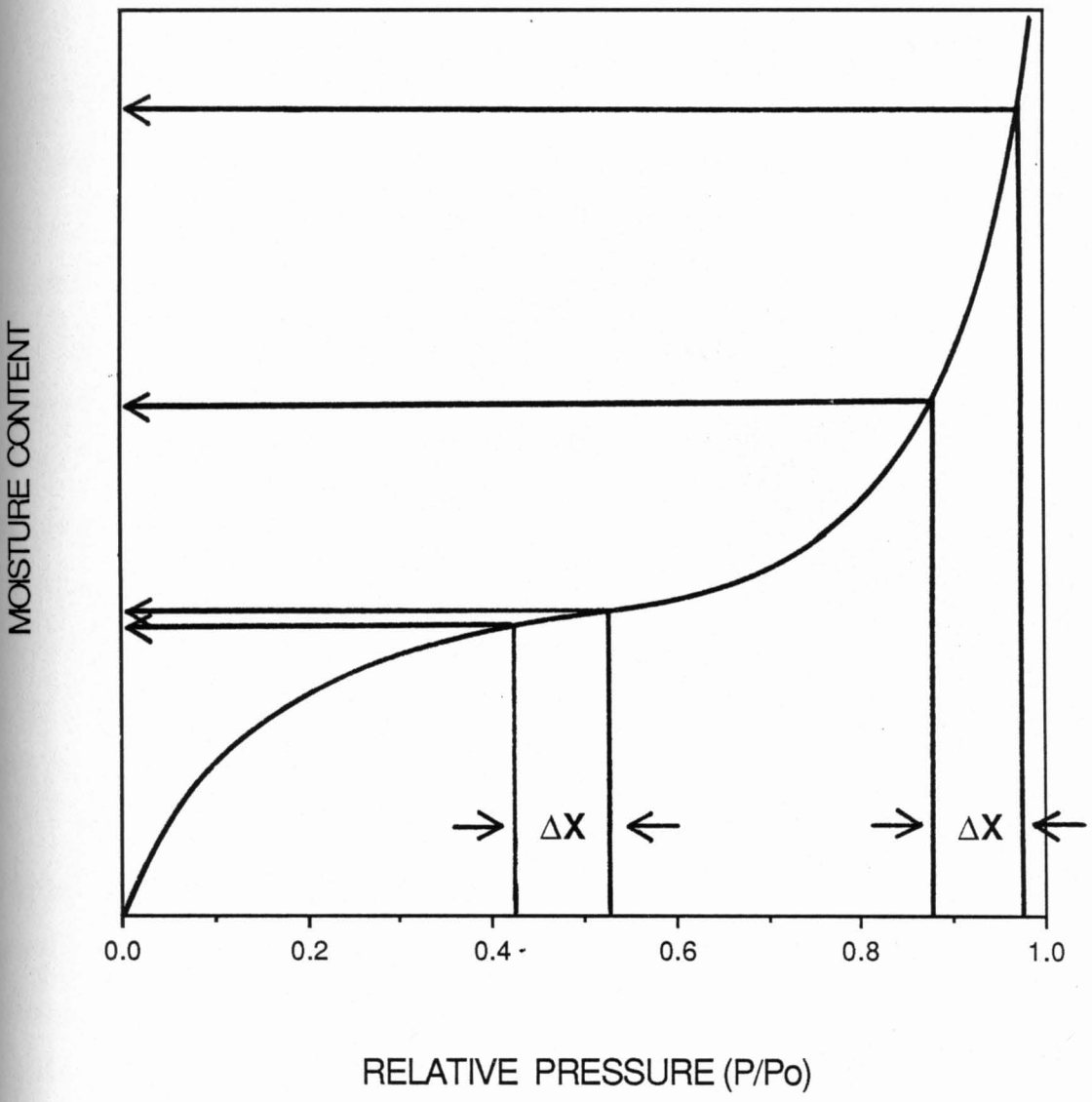

Figure 17: Error associated with extreme portions of isotherm.

A small experimental error, ΔX, in the intermediate range of the isotherm, where the moisture content is not significantly changing as relative pressure changes, produces a minimal error in the moisture content estimated for the component. An identical experimental error, however, in the upper or lower extremes of the isotherm, where the moisture content is rapidly changing, may produce a considerable error in the estimated moisture content of the component. Further, error may also result from curve fitting of the GAB equation or any other equation in these extreme regions of the isotherm. It is these regions in which a relatively poorer fit usually occurs.

Errors attributable to extremes can be clearly seen in Tables 7 and 8 where predicted versus experimental results show significant deviations when the initial relative humidities are in the very high or very low isotherm regions.

2. Error due to hysteresis. Figure 18 shows the hysteresis loop as that area between the main branches of the sorption (curve A) and desorption (curve B) isotherms. As described previously, each of these sigmoidal shaped curves can be described by the GAB equation where GAB constants are separately obtained for each curve. So long

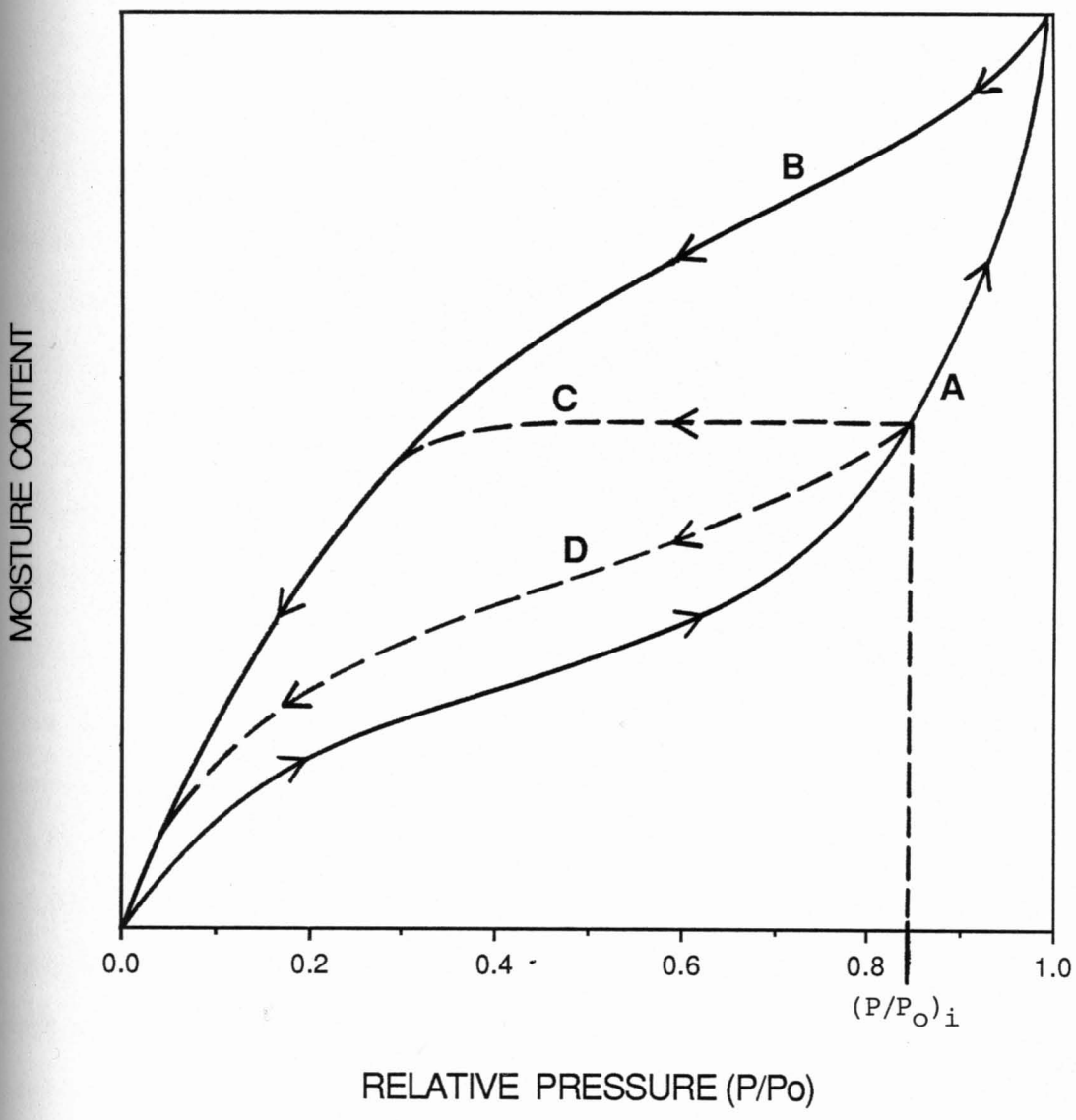

Figure 18: Graphical representation of desorption beginning at an intermediate point along the sorption isotherm.

as desorption begins from the highest point along the sorption curve (i.e., $P/P_o=1$), then the component undergoing desorption in the SDMT model can accurately be described by the desorption GAB constants. However, in most practical circumstances, sorption will not reach the highest point, but will instead reach some intermediate relative pressure, $(P/P_o)_i$, giving rise to a different desorption isotherm. Therefore, some important questions to ask are: What is the appearance of the desorption curve beginning at $(P/P_o)_i$? Does desorption follow curve C, whereby a constant moisture content is maintained as the relative pressure is decreased until the main desorption curve is reached, or does it follow curve D, whereby a unique desorption curve results? Whichever is the case, it should be apparant that desorption beginning at an intermediate point along the sorption curve cannot be accurately represented by the GAB constants for the main desorption curve. The error associated with these curves should become more pronounced with components exhibiting higher degrees of hysteresis.

Figures 19, 20, and 21 show the results of desorption mini-isotherms for microcrystalline cellulose, corn starch, and gelatin capsules, respectively. (Since the desiccant characteristics of silica gel only allowed sorption in these

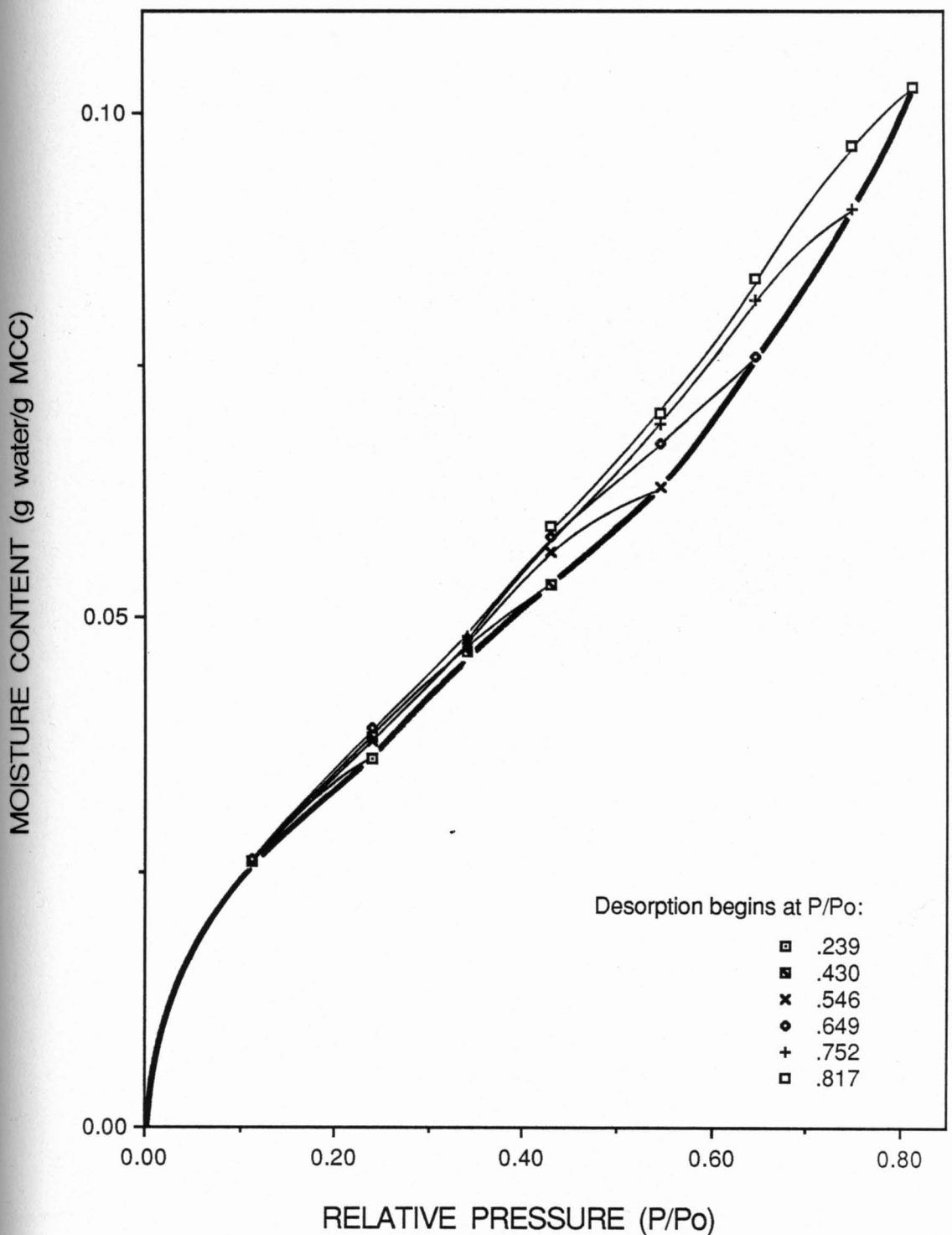

Figure 19: Desorption mini-isotherms for microcrystalline cellulose. Desorption beginning at intermediate points along the main sorption isotherm (bold line).
Lines drawn by eye for convenience of the reader.

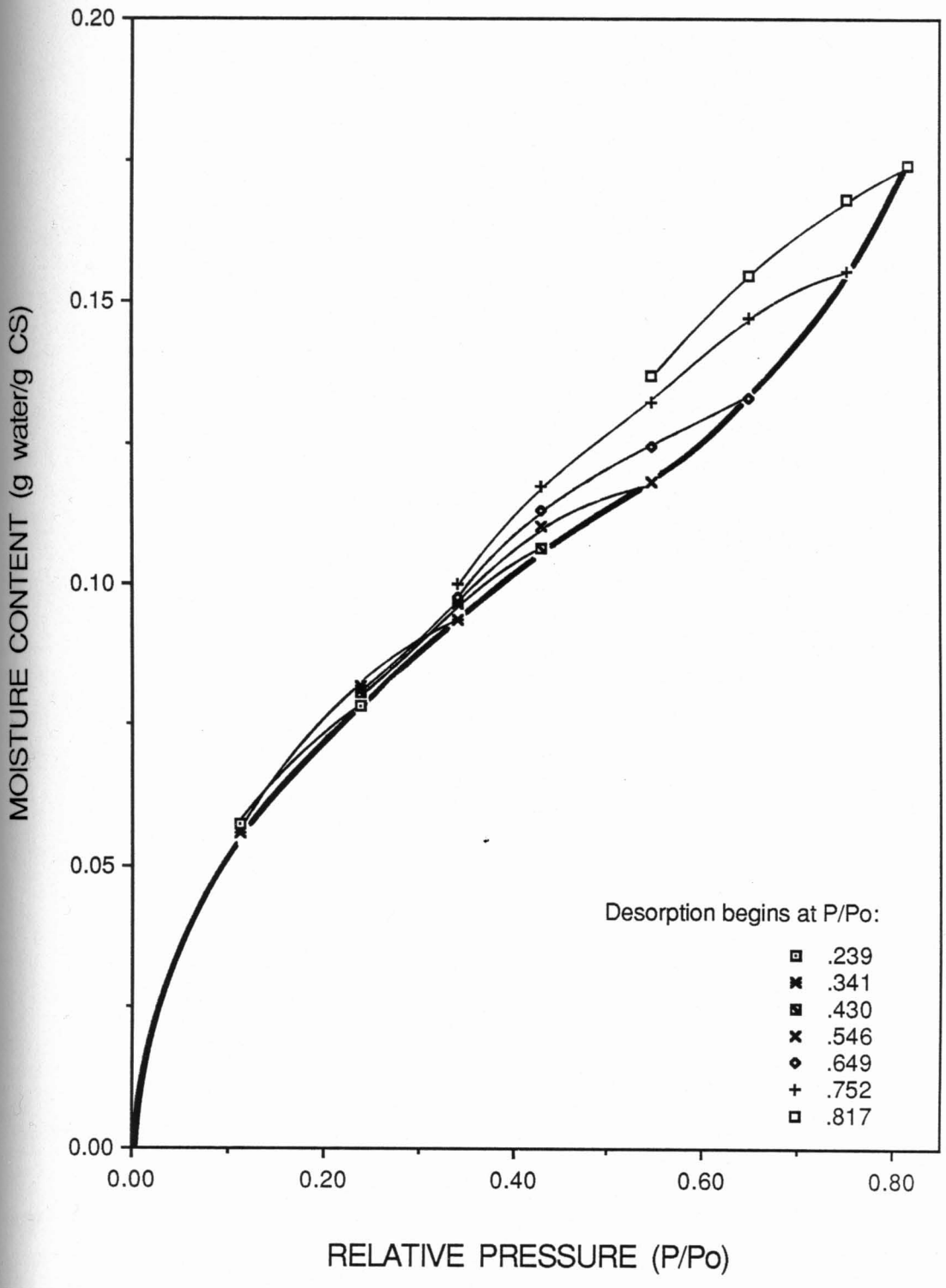

Figure 20: Desorption mini-isotherms for corn starch. Desorption beginning at intermediate points along the main sorption isotherm (bold line). Lines drawn by eye for convenience of the reader.

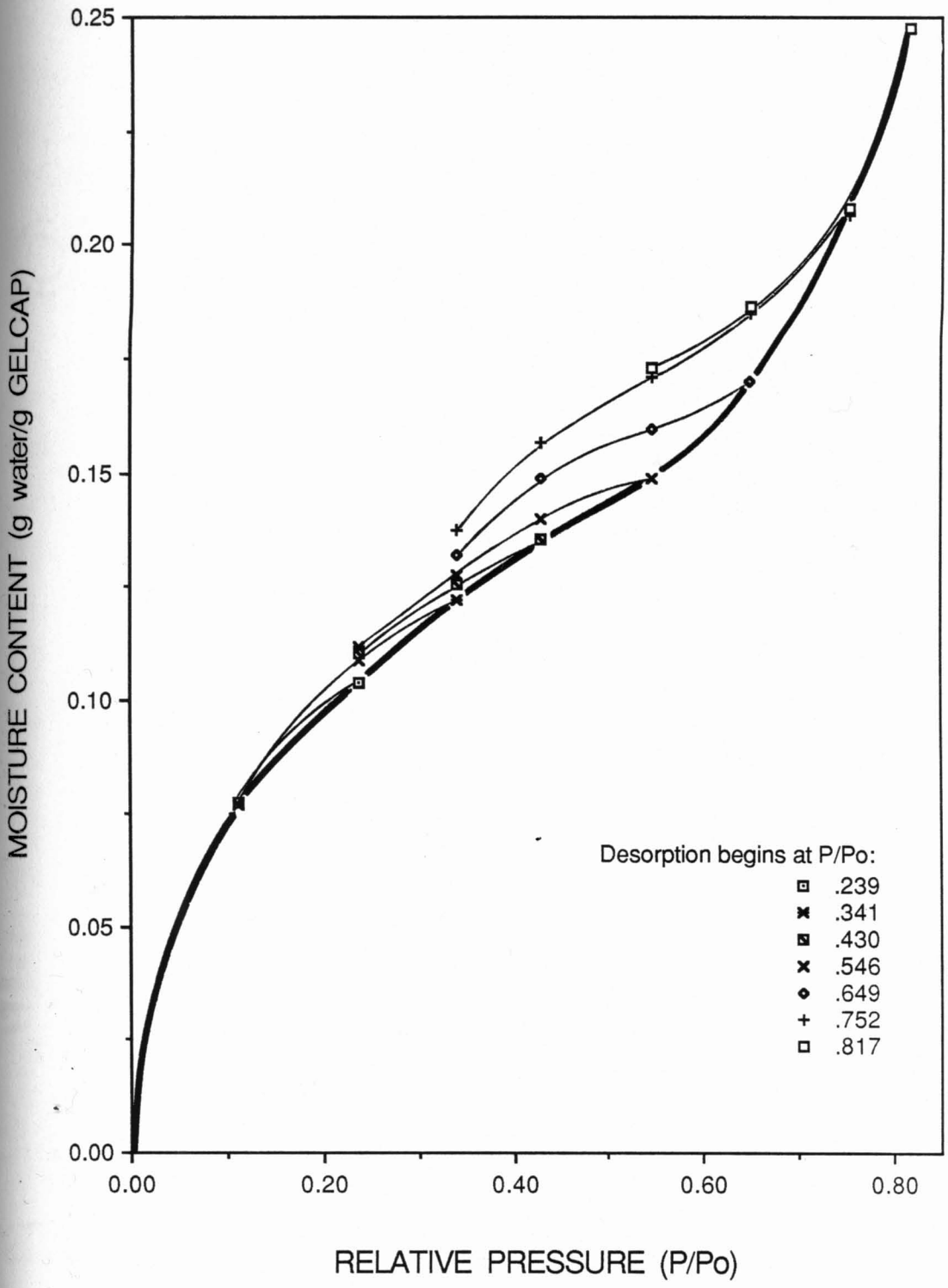

Figure 21: Desorption mini-isotherms for gelatin capsules. Desorption beginning at intermediate points along the main sorption isotherm (bold line). Lines drawn by eye for convenience of the reader.

studies, desorption mini-isotherms were not performed for this component.) Desorption isotherms were commenced from various intermediate relative pressures along the main sorption branch. From these curves, it is apparant that unique desorption curves result depending on the relative pressure at which desorption is initiated. The error which results from using GAB constants for the main desorption isotherm to describe these mini-isotherms is probably not significant, however, when compared to the error at very high and very low relative pressures.

VI. PHARMACEUTICAL APPLICATIONS

Relatively good agreement has been established between predicted and experimental values of water vapor transfer among solids in a mixture using the SDMT method of prediction. It may be of some interest to provide a few case study examples of how this method might be used in practical situations. The primary usefulness of the approach is that by knowing the moisture content, dry weight, temperature, head space volume, and water vapor sorption-desorption isotherm of each solid in the mixture, one can determine the final relative humidity over the mixture and hence the reequilibrated amount of water sorbed on each solid. More importantly, one can vary parameters such as initial dry weight, temperature, and head space volume, and by computer simulation determine which combination of conditions bring about the desired distribution of moisture among solids and vapor phase. Below are given three case studies designed to illustrate the general value of this approach.

Example 1: Capsule Formulation. Hard gelatin capsules have a critical moisture content range of about 10 to 18% water. From the water vapor sorption isotherms, it can be

shown that these moisture content values correspond to about 20 to 60% relative humidity, respectively. Capsules stored below 20% RH exhibit a drying out which results in brittleness, whereas capsules stored above 60% RH sorb sufficient water to cause softening of the capsule.

Consider the formulation given in Table 11a. One hundred gelatin capsules are to be filled with a mixture of 100mg microcrystalline cellulose and 100mg corn starch, and then stored in a 60ml tightly closed glass container. The head space volume in the container is estimated to be 15ml. The capsules have been previously stored in an environmentally controlled room at 50.0% RH giving an initial water content of 15%. Microcrystalline cellulose and corn starch, however, have not been stored under controlled conditions, and the initial relative humidity associated with these components is 90.0% RH giving initial water contents of 14 and 27%, respectively. After combining these components, it can be intuitively determined that the final equilibrium relative humidity of the product will be somewhere between 50.0 and 90.0% RH. In fact the SDMT model, using known GAB constants for these components, predicts 82.1% RH. Since 82.1% RH is in excess of the upper critical limit (60%) for the capsules, it is expected that capsule instability due to softening will occur. It is

Table 11a

Final Equilibrium Relative Humidity
for 100 Gelatin Capsules Filled with
Microcrystalline Cellulose and Corn Starch Mixture (1:1)

COMPONENT	INITIAL %RH	INITIAL DRY WEIGHT
Gelatin capsules	50.0	4.0g
Micro. cellulose	90.0	10.0g
Corn starch	90.0	10.0g

Temperature = 23°C, Head space volume = 15ml
Final Equilibrium Relative Humidity* = 82.1%

Table 11b

Increase of Head Space Volume to Reduce
Final Equilibrium Relative Humidity

HEAD SPACE VOLUME (ml)	FINAL EQUILIBRIUM RELATIVE HUMIDITY*
15	82.1
1,000	81.9
10,000	80.4
100,000	65.2
130,000	60.6

Table 11c

Addition of Silica Gel+ to Reduce the
Final Equilibrium Relative Humidity

QUANTITY OF SILICA GEL ADDED (grams)	FINAL EQUILIBRIUM RELATIVE HUMIDITY*
2.0	73.2
4.0	63.4
4.7	60.0
15.0	26.3
19.8	20.0
22.0	18.1

* Predicted values using SDMT model.
+ 0% initial relative humidity was used for silica gel.

desirable, therefore, to reduce the final equilibrium relative humidity in the container to within the acceptable capsule range.

One possible method of reducing the relative humidity within the container is by increasing the head space volume, since moisture will desorb from the components and into the increased volume. Table 11b shows, however, that the head space volume needed to reduce the relative humidity below 60% must exceed 130 liters.

A better method to effect a reduction in the relative humidity is the incorporation of a desiccant (e.g., silica gel) in the product container. A sufficient quantity of silica gel must be added to reduce the relative humidity below 60%, however not so much that the relative humidity is reduced below 20%. Table 11ç shows the predicted final equibrium relative humidities using the SDMT model for various quantities of silica gel. As can be observed from the table, the quantity of silica gel used should be between 4.7 and 19.8 grams to maintain the final equilibrium relative humidity within the acceptable capsule range of 20 to 60% RH.

Example 2. Stability of a Drug Hydrate. Figure 22 presents the moisture isotherm of an arbitrary drug compound

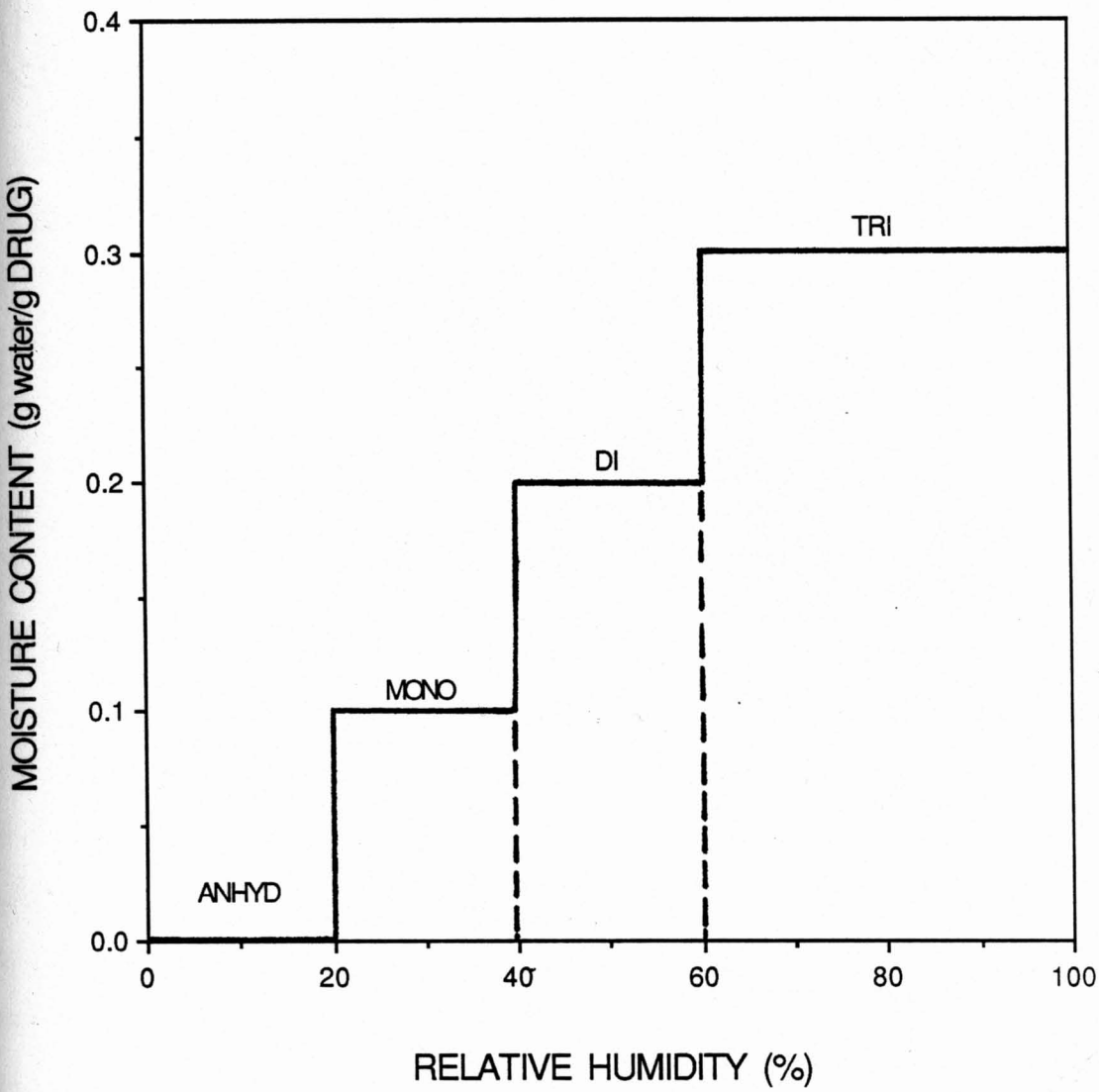

Figure 22: Moisture sorption isotherm for arbitrary drug hydrate.

which may exist in one of four hydrate forms: anhydrous, monohydrate, dihydrate, or trihydrate. The most stable form of the drug is the dihydrate which exists over the relative humidity range of 40 to 60%.

Suppose a tablet formulation is to be prepared containing 25mg of drug in a total tablet weight of 100mg. The remaining 75mg is to be composed of microcrystalline cellulose and corn starch in any proportion. One hundred tablets are to be stored in a 50ml tightly sealed glass container with a head space volume estimated to be 30ml. Since the drug has a critical moisture range between 40 and 60% RH, the optimum relative humidity for formulation is assumed to be 50%. Thus, the drug is stored in a desiccator over a saturated salt solution at 50% RH so as to maintain the dihydrate. Given that the initial moisture contents, as determined by loss-on-drying, for microcrystalline cellulose and corn starch are 4.4% and 17.0%, respectively, what combination of these two excipients will produce a final equilibrium relative humidity of 50%?

Table 12a provides the initial information necessary to formulate a container of 100 tablets. For the drug, the amount of water associated with the solid is always equal to 0.5g water at 50% RH (2.5g drug x 0.2g water per g of drug at 50% RH). Since the initial percent water is given for

Table 12a

Initial Conditions for Tablet Formulation
Containing Drug Hydrate

COMPONENT	INITIAL $\%H_2O$ (%RH)		INITIAL DRY WEIGHT[+]
Drug	20.0	(50)	2.5g
Micro. cellulose	4.4	(40)	{ total
Corn starch	17.0	(70)	{ 7.5g

Temperature = 23°C, Head space volume = 30ml

Table 12b

Final Equilibrium Relative Humidity
Using Various Combinations of
Microcrystalline Cellulose and Corn Starch

COMPOSITION (grams)			FINAL EQUILIBRIUM
MCC	CS	DRUG	RELATIVE HUMIDITY*
7.0	0.5	2.5	42.9
6.0	1.5	2.5	47.1
5.5	2.0	2.5	48.7
5.0	2.5	2.5	50.0

[+] Per 100 tablets.
* Predicted values using SDMT model.

microcrystalline cellulose and corn starch, the amount of water for these solids can be readily determined for any initial weight without the need for equation 22.

To solve this formulation problem, the dry weights of microcrystalline cellulose and corn starch, W_A and W_B, respectively, in equation 24 need to be obtained. Since the total weight of microcrystalline cellulose and corn starch must equal 7.5 grams for 100 tablets, the following equation can be written:

$$W_B = 7.5g - W_A \qquad (41)$$

Replacing W_B in equation 24 with equation 41, an iterative process can be used which varies the value of W_A until the desired final relative pressure, P/P_o, of 0.5 is obtained.

Table 12b shows results obtained using various combinations of microcrystalline cellulose and corn starch. A final composition of 5.0g microcrystalline cellulose, 2.5g corn starch, and 2.5g drug provides the desired final relative humidity condition of 50%.

Example 3: Lyophilized Formulation of Low Moisture Drugs. In example 1 it was shown that an increase in the head space volume was an impractical method for reducing the relative humidity to an acceptable level. This was so because the amount of moisture in the vapor space was negligible when compared to the moisture associated with the solids. The same is not true, however, for crystalline solids having relatively low surface areas, and hence take up only very small amounts of water. For example Kontny, Grandolfi, and Zografi (67) showed that crystalline sodium chloride takes up no more than about 5×10^{-5} g H_2O/g NaCl at a relative pressure near its deliquescence point ($P/P_o \approx .75$). In this case the vapor state may provide a significant source of moisture.

For this example, consider a mixture of two solids, component A and component B, found in a lyophilized product each of which contains very small amounts of moisture. Let us assume the following isotherm constants from the GAB equation:

	W_m	C_G	K
Component A	.00754	.0322	.168
Component B	.00962	-20.1	1.27

Each of these solids is water soluble and has the following relative humidity at saturation and 20°C:

Component A $RH_o = 75\%$

Component B $RH_o = 84\%$

When mixed together, however, the equilibrium relative humidity above a saturated solution of these solids falls to 63% as predicted by Ross (equation 11) for any mixture of water soluble solids. Hence, in order to maintain acceptable stability in a dosage form containing these components, the equilibrium relative humidity must be kept below 63%.

Consider a lyophilized dosage form containing 0.95g of component A and 0.05g of component B in a glass vial with an estimated 5ml head space. Following the freeze-drying process, a residual moisture content remains associated with each of the solids which produces a final relative humidity in the vial of 65%. To what size must the head space be increased such that the relative humidity is reduced below the acceptable value of 63%?

Table 13a provides the initial information needed to complete this problem. Using equation 24, it is necessary to solve for the term V_T, the total head space volume, at $P/P_o = .63$. Table 13b gives the final equilibrium relative humidity results for various head space volumes. Clearly, a

Table 13a

Initial Conditions for Lyophilized Dosage Form

COMPONENT	INITIAL %RH	INITIAL DRY WEIGHT
Component A	65.0	0.95g
Component B	65.0	0.05g

Temperature = 20°C, Head space volume = 5ml

Table 13b

Increase of Head Space Volume to Reduce Final Equilibrium Relative Humidity

HEAD SPACE VOLUME(ml)	FINAL EQUILIBRIUM RELATIVE HUMIDITY*
5	65.0
10	64.7
20	64.1
30	63.5
38	63.0
40	62.8

* Predicted values using SDMT model.

vial providing a head space in excess of 38ml is necessary to maintain an acceptable relative humidity below 63%.

VII. CONCLUSIONS

The empirical approach first used by Salwin and Slawson for predicting the final equilibrium relative humidity above a mixture of components was modified in the present work to produce the Sorption-Desorption Moisture Transfer (SDMT) model. This model utilized an equation describing the moisture isotherm so that the moisture content of a particular component could be determined over the entire relative humidity range as a function of various parameters. The SDMT model provided reasonable results for moisture transfer among several components when only transmission through the vapor state was assumed to take place. It was shown that by including the desorption isotherm and vapor state moisture, improved results were obtained as compared to previous models.

It should be emphasized that although this work primarily used the GAB equation to describe the moisture isotherms (and indeed a wide number of excipients are described by the GAB equation as given in Appendix 5), this is not a limitation of the model as shown when silica gel was a constituent of the mixture. The iterative process used for the predictive calculation is flexible enough to allow the incorporation of any equation which describes a

moisture isotherm.

Most importantly, the SDMT model has the significant advantage over previous work in that simulations are possible for multiple component systems. In this way *a priori* predictions can be obtained for final equilibrium moisture conditions, thus minimizing unnecessary preliminary experimentation. This should provide a tool for the pharmaceutical formulator to minimize much of the empiricism in formulating moisture-sensitive solid dosage forms. The only data necessary in proceeding with the model are initial conditions such as dry weight, moisture content, temperature, head space volume, and water vapor sorption-desorption isotherms for all components.

VIII. APPENDICES

Appendix 1. Constant terms for equation 25.

$$C_1 = \frac{1}{K_B(Cg_B-1)} - \frac{1}{K_B} + \frac{1}{K_A(Cg_A-1)} - \frac{1}{K_A} - \frac{M_T RT}{VP_o(18)}$$

$$C_2 = \frac{1}{K_A(Cg_A-1)}\left[\frac{1}{K_B(Cg_B-1)} - \frac{1}{K_A} - \frac{1}{K_B}\right] - \frac{1}{K_B(Cg_B-1)}\left[\frac{1}{K_B} + \frac{1}{K_A}\right] + \frac{1}{K_A K_B}$$

$$- \frac{RT}{VP_o(18)}\left[\frac{W_A Wm_A Cg_A}{K_A(Cg_A-1)} + \frac{W_B Wm_B Cg_B}{K_B(Cg_B-1)}\right] + \frac{M_T RT}{VP_o(18)}\left[\frac{1}{K_B}\left(1 - \frac{1}{(Cg_B-1)}\right) + \frac{1}{K_A}\left(1 - \frac{1}{(Cg_A-1)}\right)\right]$$

$$C_3 = \frac{\frac{VP_o(18)}{RT}\left[K_A(Cg_A-2)+K_B(Cg_B-2)\right] + W_A Wm_A Cg_A K_A K_B(Cg_B-2) + W_B Wm_B Cg_B K_A K_B(Cg_A-2) + M_T\left[K_A(Cg_A-1)(K_A+K_B(2-Cg_B)) + K_B(K_A+K_B)(Cg_B-1) - K_A K_B\right]}{(K_A K_B)^2(Cg_A-1)(Cg_B-1)\frac{VP_o(18)}{RT}}$$

$$C_4 = \frac{\frac{VP_o(18)}{RT} + W_A Wm_A Cg_A K_A + W_B Wm_B Cg_B K_B + M_T\left[K_A(2-Cg_A) + K_B(2-Cg_B)\right]}{(K_A K_B)^2(Cg_A-1)(Cg_B-1)\frac{VP_o(18)}{RT}}$$

$$C_5 = \frac{M_T RT}{(K_A K_B)^2(Cg_A-1)(Cg_B-1)\,VP_o(18)}$$

Appendix 2. BASIC computer program to calculate moisture transfer using Newton's method.

```
10  REM    ITERATION PROGRAM FOR
11  REM    TWO COMPONENT SYSTEM
12  REM    USING NEWTON'S METHOD
17  REM
20  REM    WRITTEN BY G. GRANDOLFI

21  REM         MARCH 14, 1986
30  :
40  :
50 R = 82.0562
60  HOME : VTAB 15
70 N = 2
80  DIM V(N),W(N),RP(N),WM(N),CG(
    N),K(N),MS(N),MV(N)
90  HOME : VTAB 15
100  INPUT "TEMPERATURE (centigra
    de)? ";T
110 T = T + 273.15
120  HOME : VTAB 15
130  INPUT "Po AT THIS TEMPERATUR
    E ? ";P0
135 :
136 :
137  REM  ENTER PERTINENT DATA FO
    R EACH COMPONENT
138 :
140  PR# 0
150  FOR X = 1 TO N
160  HOME : VTAB 10
170  FLASH
180  PRINT "INFORMATION FOR COMPO
    NENT ";X
190  NORMAL
200  VTAB 13
210  INPUT "INITIAL VOLUME (ml) "
    ;V(X)
220  INPUT "INITIAL DRY WEIGHT (g
    rams) ";W(X)
230  INPUT "INITIAL RELATIVE PRES
    SURE ";RP(X)
240  INPUT "GAB CONSTANTS: Wm, Cg
    , K ";WM(X),CG(X),K(X)
```

(Appendix 2 continued)

```
250  NEXT X
300  :
310  :
320  REM  PRINT OUT THE INITIAL I
     NFORMATION
330  :
340  PR# 1
350  PRINT "------------------"
360  PRINT "   INITIAL DATA"
370  PRINT "------------------"
390  PRINT "TEMPERATURE = ";T - 2
     73.15;" deg C"
400  PRINT "Po AT ";T - 273.15;"
     deg C = ";P0
410  PRINT
420  FOR X = 1 TO N
430  PRINT "COMPONENT ";X
450  PRINT "      INITIAL VOLUME =
      ";V(X)
460  PRINT "      INITIAL DRY WEIG
     HT = ";W(X)
470  PRINT "      INITIAL RELATIVE
      PRESSURE = ";RP(X)
480  PRINT "      Wm = ";WM(X)
490  PRINT "      Cg = ";CG(X)
500  PRINT "      K  = ";K(X)
510  PRINT
520  NEXT X
1000 :
1010 :
1020  REM  FOR EACH COMPONENT, CO
     MPUTE THE WATER ON THE SOLID
      AND IN THE VAPOR SPACE
1030 :
1040  PRINT
1050  PRINT "--------------------
     -"
1060  PRINT "   CALCULATED DATA"
1070  PRINT "--------------------
     -"
1080 MT = 0
1090  FOR X = 1 TO N
1100 P = RP(X)
1110  GOSUB 9500
1120  GOSUB 9000
1130 MT = MT + MS(X) + MV(X)
1140  PRINT "INITIAL AMOUNT OF WA
     TER FOR COMPONENT ";X
1150  PRINT "      MASS OF WATER O
     N SOLID = ";MS(X);" grams"
```

(Appendix 2 continued)

```
1160  PRINT "      MASS OF WATER I
     N VAPOR = ";MV(X);" grams"
1170  PRINT
1180  NEXT X
1200  PRINT "TOTAL WATER IN SYSTE
     M = ";MT;" grams"
2000 :
2010 :
2020  REM  BEGIN CALCULATIONS FOR
      NEW EXPANDED VOLUME
2025 :
2030  PR# 0
2040  HOME : VTAB 15
2050  INPUT "EXPAND TO A NEW TOTA
     L VOLUME OF ?? ";VT
2051  INPUT "WHICH COMPONENT TO D
     ESORB (1 or 2)?";Y
2053  INPUT "Wm, Cg, K  FOR DESOR
     PTION";WM(Y),CG(Y),K(Y)
2060  PR# 1
2070  PRINT
2080  PRINT "SYSTEM EXPANSION TO
     NEW TOTAL VOLUME OF ";VT;" m
     l"
2081  PRINT "COMPONENT ";Y;" TO D
     ESORB ON EXPANSION"
2082  PRINT "      Wm = ";WM(Y)
2083  PRINT "      Cg = ";CG(Y)
2084  PRINT "      K  = ";K(Y)
8000 :
8010 :
8020  REM  BEGIN NEWTON'S METHOD
8030 :
8040 C1 = (1 / (K(2) * (CG(2) - 1
     ))) - (1 / K(2)) + (1 / (K(1
     ) * (CG(1) - 1))) - (1 / K(1
     )) - ((MT * R * T * 760) / (
     VT * P0 * 18))
8050 D1 = ((1 / (K(1) * (CG(1) -
     1))) * ((1 / (K(2) * (CG(2) -
     1))) - (1 / K(2)) - (1 / K(1
     ))))
8060 D2 = ((1 / (K(2) * (CG(2) -
     1))) * ((1 / K(2)) + (1 / K(
     1))))
8070 D3 = (1 / (K(1) * K(2)))
8080 D4 = ((R * T * 760) / (VT *
     P0 * 18)) * (((W(1) * WM(1) *
     CG(1)) / (K(1) * (CG(1) - 1)
     )) + ((W(2) * WM(2) * CG(2))
      / (K(2) * (CG(2) - 1))))
```

(Appendix 2 continued)

```
8090 D5 = ((MT * R * T * 760) / (
     VT * P0 * 18)) * (((1 / K(2)
     ) * (1 - (1 / (CG(2) - 1))))
      + ((1 / K(1)) * (1 - (1 / (
     CG(1) - 1)))))
8100 C2 = D1 - D2 + D3 - D4 + D5
8110 E1 = ((VT * P0 * 18) / (R *
     T * 760)) * ((K(1) * (CG(1) -
     2)) + (K(2) * (CG(2) - 2)))
8120 E2 = (W(1) * WM(1) * CG(1) *
     K(1) * K(2)) * (CG(2) - 2)
8130 E3 = (W(2) * WM(2) * CG(2) *
     K(1) * K(2)) * (CG(1) - 2)
8140 E4 = ((K(1) * (CG(1) - 1)) *
     (K(1) + (K(2) * (2 - CG(2)))
     )) + (K(2) * (K(1) + K(2)) *
     (CG(2) - 1)) - (K(1) * K(2))

8150 E5 = ((K(1) ^ 2) * (K(2) ^ 2
     ) * VT * P0 * 18 * (CG(1) -
     1) * (CG(2) - 1)) / (R * T *
     760)
8160 C3 = (E1 + E2 + E3 + (MT * E
     4)) / E5
8170 F1 = ((VT * P0 * 18) / (R *
     T * 760)) + (W(1) * WM(1) *
     CG(1) * K(1)) + (W(2) * WM(2
     ) * CG(2) * K(2))
8180 F2 = MT * ((K(1) * (2 - CG(1
     ))) + (K(2) * (2 - CG(2))))
8190 C4 = (F1 + F2) / E5
8200 C5 = MT / E5
8300  PRINT : PRINT
8309  PRINT "-------------------
     ------------"
8310  PRINT "   NEWTON APPROXIMAT
     ION METHOD"
8311  PRINT "-------------------
     ------------"
8320  FOR J = 1 TO 0 STEP  - 0.1
8325 Z = (J ^ 5) + (C1 * (J ^ 4))
      + (C2 * (J ^ 3)) + (C3 * (J
      ^ 2)) + (C4 * J) - C5
8330  IF Z <  = 0 THEN 8380
8335  NEXT J
8380 X = J + 0.1
8393  PRINT "X= ";X
8400  FOR I = 1 TO 10
8410 G = (X ^ 5) + (C1 * (X ^ 4))
      + (C2 * (X ^ 3)) + (C3 * (X
      ^ 2)) + (C4 * X) - C5
```

(Appendix 2 continued)

```
8420 G1 = (5 * (X ^ 4)) + (4 * C1
      * (X ^ 3)) + (3 * C2 * (X ^
     2)) + (2 * C3 * X) + C4
8430 X = X - (G / G1)
8440  REM  PRINT I,X
8450  NEXT I
8451  PRINT
8452  PRINT "CALCULATED FINAL REL
     ATIVE PRESSURE = ";X
9000 :
9010 :
9020  REM  IDEAL GAS LAW SUBROUTI
     NE
9030  REM  RETURNS MASS IN VAPOR
     STATE
9040 :
9050 MV(X) = (P * P0 * V(X) * 18)
      / (760 * R * T)
9060  RETURN
9500 :
9510 :
9520  REM  GAB SUBROUTINE
9530  REM  RETURNS MASS OF WATER
     ON SOLID OF COMPONENT N
9540 :
9550 MS(X) = (W(X) * WM(X) * CG(X
     ) * K(X) * P) / ((1 - (K(X) *
     P)) * (1 - (K(X) * P) + (CG(
     X) * K(X) * P)))
9560  RETURN
```

Appendix 3. BASIC computer program to calculate moisture transfer using iteration technique.

```
10  REM    ITERATION PROGRAM FOR
11  REM    MULTICOMPONENT SYSTEM
12  REM
13  REM    WRITTEN BY G. GRANDOLFI

14  REM          MARCH 14, 1986
15  REM
20  REM    MODIFIED OCT 10, 1986
21  REM    MODIFIED NOV 12, 1986
25  :
30  :
35  :
40 Q = 9
41  DIM C1$(Q),T1(Q),P1(Q),W1(Q),
     C1(Q),K1(Q)
43  FOR X = 1 TO Q
45  READ C1$(X),T1(X),P1(X),W1(X)
     ,C1(X),K1(X)
47  NEXT X
50 R = 82.0562
60  HOME : VTAB 15
70  INPUT "NUMBER OF COMPONENTS T
     O BE USED ? ";N
80  DIM V(N),W(N),RP(N),WM(N),CG(
     N),K(N),MS(N),MV(N),T(N),P0(
     N),C$(N)
135 :
136 :
137  REM  ENTER PERTINENT DATA FO
     R EACH COMPONENT
138 :
140  PR# 0
150  FOR X = 1 TO N
160  HOME : VTAB 5
170  FLASH : PRINT "INFORMATION F
     OR COMPONENT ";X: NORMAL
175  PRINT : GOSUB 9500
180  HOME : VTAB 5
190  FLASH : PRINT "INFORMATION F
     OR COMPONENT ";X: NORMAL
200  PRINT : PRINT "COMPONENT = "
     ;C$(X): PRINT "TEMP = ";T(X)
```

(Appendix 3 continued)

```
204  PRINT "Po = ";P0(X): PRINT "
     Wm = ";WM(X)
206  PRINT "Cg = ";CG(X): PRINT "
     K = ";K(X): PRINT
210  INPUT "INITIAL VOLUME (ml) "
     ;V(X)
220  INPUT "INITIAL DRY WEIGHT (g
     rams) ";W(X)
230  INPUT "INITIAL RELATIVE PRES
     SURE ";RP(X)
250  NEXT X
300  :
310  :
320  REM  PRINT OUT THE INITIAL I
     NFORMATION
330  :
340  PR# 1
350  PRINT "------------------"
360  PRINT "    INITIAL DATA"
370  PRINT "------------------"
420  FOR X = 1 TO N
430  PRINT "COMPONENT ";X;" = ";C
     $(X)
435  PRINT "      TEMP = ";T(X)
440  PRINT "      Po = ";P0(X)
450  PRINT "      INITIAL VOLUME =
      ";V(X)
460  PRINT "      INITIAL DRY WEIG
     HT = ";W(X)
470  PRINT "      INITIAL RELATIVE
      PRESSURE = ";RP(X)
480  PRINT "      Wm = ";WM(X)
490  PRINT "      Cg = ";CG(X)
500  PRINT "      K  = ";K(X)
510  PRINT
520  NEXT X
1000 :
1010 :
1020  REM  FOR EACH COMPONENT, CO
     MPUTE THE WATER ON THE SOLID
      AND IN THE VAPOR SPACE
1030 :
1040  PRINT : PRINT
1050  PRINT "--------------------
     -"
1060  PRINT "    CALCULATED DATA"
1070  PRINT "--------------------
     -"
1080 MT = 0
1090  FOR X = 1 TO N
1100 P = RP(X)
```

(Appendix 3 continued)

```
1110  GOSUB 9000
1115  IF K(X) = 0 THEN 1125
1120  GOSUB 8000
1121  GOTO 1130
1125  GOSUB 7500
1130 MT = MT + MS(X) + MV(X)
1140  PRINT "INITIAL AMOUNT OF WA
      TER FOR COMPONENT ";X;" = ";
      C$(X)
1150  PRINT "      MASS OF WATER O
      N SOLID = ";MS(X);" grams"
1160  PRINT "      MASS OF WATER I
      N VAPOR = ";MV(X);" grams"
1170  PRINT
1180  NEXT X
1190  PRINT
1200  PRINT "TOTAL WATER IN SYSTE
      M = ";MT;" grams"
1201  PRINT : PRINT
1202  PRINT "--------------------
      ------"
1203  PRINT "   COMPONENTS TO DES
      ORB"
1204  PRINT "--------------------
      ------"
2000 :
2010 :
2020  REM  BEGIN CALCULATIONS FOR
       NEW EXPANDED VOLUME
2025 :
2030  PR# 0
2040  HOME : VTAB 15
2050  INPUT "EXPAND TO A NEW TOTA
      L VOLUME OF ?? ";VT
2051  FOR X = 1 TO N
2053  PRINT "WILL COMPONENT ";X;"
       = ";C$(X);" DESORB??"
2055  INPUT "(Y/N)";A$
2060  IF A$ = "Y" THEN 2064
2062  IF A$ = "N" THEN 2090
2063  GOTO 2055
2064  HOME : VTAB 5: GOSUB 9500
2066  PR# 1
2075  PRINT "COMPONENT ";X;" = "C
      $(X)
2080  PRINT "      TEMP = ";T(X)
2081  PRINT "      Po = ";P0(X)
2082  PRINT "      Wm = ";WM(X)
2083  PRINT "      Cg = ";CG(X)
2084  PRINT "      K  = ";K(X)
2085  PR# 0
```

(Appendix 3 continued)

```
2090  NEXT X
2100  PR# 1
2110  PRINT
2120  PRINT "SYSTEM EXPANSION TO
      NEW TOTAL VOLUME OF ";VT;" m
      l"
2200 :
2210 :
2220  REM  BEGIN THE ITERATION
2230 :
2240 PNOW = .5
2250 PHIGH = 1.0
2260 PLOW = 0.0
3000 P = PNOW
3010 MCALC = 0
3020  FOR X = 1 TO N
3025  IF K(X) = 0 THEN 3035
3030  GOSUB 8000
3031  GOTO 3040
3035  GOSUB 7500
3040 MCALC = MCALC + MS(X)
3050  NEXT X
3059 X = 1
3060 V(X) = VT
3070  GOSUB 9000
3080 MCALC = MCALC + MV(X)
3200  IF  INT (MCALC * 100000000)
      =  INT (MT * 100000000) THEN
      7000
3210  IF  INT (MCALC * 100000000)
      >  INT (MT * 100000000) THEN
      4000
3220 PLOW = PNOW
3230  GOTO 4100
4000 PHIGH = PNOW
4100 PNOW = (PLOW + PHIGH) / 2
4101  PRINT PNOW
4110  GOTO 3000
7000 :
7010 :
7020  REM  FINAL RELATIVE PRESSUR
      E HAS BEEN CALCULATED
7030 :
7040  PRINT : PRINT
7050  PRINT "-------------------
      -------------------------"
7060  PRINT "CALCULATED FINAL REL
      ATIVE PRESSURE = ";PNOW
7070  PRINT "-------------------
      -------------------------"
```

(Appendix 3 continued)

```
7100  END
7497 :
7498 :
7499 :
7500  REM  LANGMUIR SUBROUTINE
7501  REM  RETURNS MASS OF WATER
     ON COMPONENT N
7502 :
7510 MS(X) = (W(X) * WM(X) * CG(X
     ) * P) / (1 + (CG(X) * P))
7520  RETURN
8000 :
8010 :
8020  REM  GAB SUBROUTINE
8030  REM   RETURNS MASS OF WATER
      ON COMPONENT N
8040 :
8050 MS(X) = (W(X) * WM(X) * CG(X
     ) * K(X) * P) / ((1 - (K(X) *
     P)) * (1 - (K(X) * P) + (CG(
     X) * K(X) * P)))
8060  RETURN
9000 :
9010 :
9020  REM  IDEAL GAS LAW SUBROUTI
     NE
9030  REM  RETURNS MASS IN VAPOR
     STATE
9040 :
9050 MV(X) = (P * P0(X) * V(X) *
     18) / (760 * R * (T(X) + 273
     .15))
9060  RETURN
9400 :
9410 :
9420 :
9500  REM    LIST THE GAB CONSTAN
     TS
9510  PRINT "LINE COMPONENT
      TEMP"
9520  PRINT "---- ---------
      ----"
9530  FOR I = 1 TO Q
9540  PRINT  TAB( 2);I; TAB( 6);C
     1$(I); TAB( 23);T1(I)
9550  NEXT I
9560  PRINT : INPUT "CHOOSE LINE
     # FOR THIS COMPONENT";L
```

(Appendix 3 continued)

```
9570  IF L < 1 OR L > Q THEN 9560

9580 C$(X) = C1$(L):T(X) = T1(L):
     P0(X) = P1(L)
9590 WM(X) = W1(L):CG(X) = C1(L):
     K(X) = K1(L)
9600  RETURN
9700 :
9710 :
9720 :
9900  REM   CHARACTER STRING MAX=
     15
9910  REM   CHANGE LINE 40 FOR "Q
     "
9920  DATA  "MCC-ADS-MK",20,17.53
     5,.0299,55.7,.870
9930  DATA  "MCC-DES-MK",20,17.53
     5,.0429,24.7,.820
9935  DATA  "MCC-ADS-MK",25,23.75
     6,.0285,49.5,.893
9936  DATA  "MCC-DES-MK",25,23.75
     6,.0403,16.6,.844
9940  DATA  "CS-ADS-MK",20,17.535
     ,.0753,67,.804
9950  DATA  "CS-DES-MK",20,17.535
     ,.114,26.9,.641
9960  DATA   "GELCAP-ADS-GG",23,2
     1.068,0.237,2.95,0.509
9965  DATA   "GELCAP-DES-GG",23,2
     1.068,0.150,25.1,0.563
9970  DATA   "SILICA-LANG",23,21.
     068,.5722,1.784,0
```

Appendix 4. Fortran non-linear regression computer program. Written by John Davis, Madison Academic Computing Center, University of Wisconsin-Madison.

```
      PARAMETER
     +NO=210,
     +NP=3,
     +LS=NO*NP+2*NO+6*NP
      DOUBLE PRECISION S(LS)
      DOUBLE PRECISION TH(NP),T(NO),Y(NO),TOL(3)
      DOUBLE PRECISION EPSMOD/1D-10/
      INTEGER IOPT(4)/0,0,0,1/,
     +     NPRT(4)/1,10,1,1/,dummy
      CHARACTER*72 TITLE
      CHARACTER*41 TITLEA
      Character*20 INFILE
      COMMON /BLK/T
      DATA TOL/0,0,0/
      DATA TH/0.0982,27.3,0.681/
      EXTERNAL EQU
      NROBS=0
      MAXMOD=800*(NP+1)
      WRITE(6,*)'Enter filename. Maximum set to 210 observations.'
      READ(5,75)INFILE
   75 FORMAT(A20)
      WRITE(6,*)'Enter title -- limit is 40 characters.'
      READ(5,80)TITLEA
      TITLE=TITLEA//' Dataset =  '//INFILE
   80 FORMAT(A72)
      OPEN(10,FILE=INFILE,STATUS='OLD')
      DO 200 I=1,NO
      READ(10,*,END=300)T(I),Y(I)
  200 NROBS=NROBS+1
  300 CONTINUE
      write(6,*)title
      CALL NREG77(NROBS,NP,TH,Y,EQU,DUMMY,EPSMOD,
     +IOPT,TOL,MAXMOD,NPRT,INFO,S,LS)
      WRITE(6,400)INFO
  400 FORMAT(' INFO VALUE IS ',I1,'. SEE PAGE 2-4 OF MANUAL.')
      STOP 1
      END
      SUBROUTINE EQU (NROBS,NP,Y,TH,R)
      DOUBLE PRECISION Y(210),TH(210),R(210),T(210),X
      COMMON /BLK/T
C     WM=TH(1),C=TH(2),K=TH(3)
      DO 20 I=1,NROBS
      X=T(I)
         R(I)=(TH(1)*TH(2)*TH(3)*X)/
     +     ((1-TH(3)*X)*(1-TH(3)*X+TH(2)*TH(3)*X))-Y(I)
   20 CONTINUE
      RETURN
      END
+
```

Appendix 5. GAB Constants for various excipients.

COMPONENT	Wm	Cg	K	Ref
Bentonite N.F.	.0494	8.38	.812	68
Cellulose Acetate Phthalate N.F.	.0495	6.94	.662	68
Cellulose, Powdered N.F.	.0569	1.65×10^4	.672	68
Croscarmellose Sodium (Acdisol)	.0936	5.81	.930	69
Croscarmellose Sodium (Acdisol)	.0622	179	.985	70
Cross Linked Dextrose (CLD-2)	.0725	448	.968	70
Cross Linked Dextrose (CLD-2)	.0979	64.7	.950	69
Dextrose U.S.P.	.0368	5.90×10^3	.939	68
Ethylcellulose N.F.	.0125	2.36	.835	68
Gelatin U.S.P.	.0671	8.17×10^3	.850	68
Hydroxpropyl Cellulose	.0420	2.46	.880	68
Hydroxypropyl Methylcellulose USP	.0299	11.1	.951	68
Magnesium Aluminum Silicate N.F.	.0481	42.3	.875	68
Magnesium Stearate N.F.	.0223	1.24×10^4	.686	68
Polyplasdone XL	.133	14.1	.708	68
Povidone U.S.P.	.0893	-4.92×10^3	.865	68
Pregelatinized Starch	.0496	-132	.860	68
Pregelatinized Starch (Starch 1500)	.0737	27.3	.801	71
Sodium Carboxymethyl Cellulose	.103	22.2	.833	68
Sodium Starch Glycolate N.F.	.0699	3.34	.891	68
Sodium Starch Glycolate (Explotab)	.0807	10.9	.975	70
Sodium Starch Glycolate (Primojel)	.0918	4.39	.983	70
Sucrose U.S.P.	7.24×10^{-4}	-4.34	1.07	68

IX. REFERENCES

1. L. Van Campen, G.L. Amidon, and G. Zografi, *J. Pharm. Sci.*, 72, 1381 (1983).

2. N.A. Armstrong and R.V. Griffiths, *Pharm. Acta Helv.*, 45, 692 (1970).

3. E.N. Hiestand, *J. Pharm. Sci.*, 55, 1325 (1966).

4. S.E. Tabibi, In Water Vapor Adsorption by Compressible Sugar and Its Effect on Powder Compressibility, Ph.D. Thesis, U. of Maryland, College Park, 1982.

5. R. Huttenrauch and J. Jacob, *Die Pharm.*, 32, 241 (1977).

6. G. Zografi and M.J. Kontny, *Pharmaceutical Research*, 3, 187 (1986).

7. K. Khan, P. Musikakhumma, and J. Warr, *Drug Dev. Ind. Pharm.*, 7, 525 (1981).

8. K. Nakabayashi, T. Shimamoto, and H. Mima, *Chem. Pharm. Bull.*, 28, 1090 (1980).

9. E. Shotton and J.E. Rees, *J. Pharm. Pharmacol.*, 18 Suppl., 160S (1966).

10. J.E. Rees and E. Shotton, *J. Pharm. Pharmacol.*, 22 Suppl., 17S (1970).

11. G.R.B. Down and J.N. McMullen, *Powder Tech.*, 42, 169 (1985).

12. N. Lordi and P. Shiromani, *Drug Dev. Ind. Pharm.*, 9, 1399 (1983).

13. N. Lordi and P. Shiromani, *Drug Dev. Ind. Pharm.*, 10, 729 (1984).

14. L.J. Leeson and A.M. Mattocks, *J. Am. Pharm. Assn.*, Sci. Ed., 47, 329 (1958).

15. J.T. Carstensen and P. Pothisiri, *J. Pharm. Sci.*, 64, 37 (1975).

16. K.S. Manudhane, A.M. Contractor, H.Y. Kim, and R.F.

Shangraw, *J. Pharm. Sci.*, 58, 616 (1969).

17. P.R. Perrier and U.W. Kesserlring, *J. Pharm. Sci.*, 72, 1072 (1983).

18. D.C. Monkhouse, *Drug Dev. Ind. Pharm.*, 10, 1373 (1984).

19. J.T. Carstensen, *J. Pharm. Sci.*, 63, 1 (1974).

20. D.C. Monkhouse and L. Van Campen, *Drug Dev. Ind. Pharm.*, 10, 1175 (1984).

21. J.T. Carstensen, *Drug Dev. Ind. Pharm.*, 10, 1277 (1984).

22. P.T. Vos and T.P. Labuza, *J. Agr. Food Chem.*, 22, 326 (1974).

23. A.W. Adamson, Physical Chemistry of Surfaces, 4th ed., John Wiley and Sons, Inc., New York, 1982.

24. S. Lowell, Introduction to Powder Surface Area, John Wiley and Sons, Inc., New York, 1979.

25. S.J. Gregg and K.S.W. Sing, Adsorption, Surface Area and Porosity, 2nd ed., Academic Press, New York, 1982.

26. I. Langmuir, *J. Am. Chem. Soc.*, 40, 1361 (1918).

27. S. Brunauer, P.H. Emmett, and E. Teller, *J. Am. Chem. Soc.*, 60, 309 (1938).

28. M. Caurie, In Water Activity: Influences on Food Quality, edited by L.B. Rockland and G.F. Stewart, Academic Press, Inc., New York, 1981.

29. A. Venkateswaren, *Chem. Rev.*, 70, 619 (1970).

30. C. van den Berg and S. Bruin, In Water Activity: Influences on Food Quality, edited by L.B. Rockland and G.F. Stewart, Academic Press, Inc., New York, 1981.

31. E.A. Guggenheim, Applications of Statistical Mechanics, Clarendon Press, Oxford, 1966.

32. R.B. Anderson, *J. Am. Chem. Soc.*, 68, 686 (1946).

33. J.H. deBoer, The Dynamic Character of Adsorption, 2nd

ed., Clarendon Press, Oxford, 1968.

34. C. van den Berg, In Vapour Sorption Equilibria and Other Water-Starch Interactions; a Physio-Chemical Approach, Ph.D. Thesis, Agricultural University Wageningen, The Netherlands, 1981.

35. M.J. Kontny, In Water Vapor Sorption Studies on Solid Surfaces, Ph.D. Thesis, University of Wisconsin, Madison, 1985.

36. Unpublished data.

37. W.P. Bryan, *Biopolymers*, 25, 1967 (1986).

38. S.M. Blaug, E. Hickman, and J.J. Lach, *J. Am. Pharm. Assn.*, 47, 54 (1958).

39. N.A. Peppas and R. Khanna, *Polym. Eng. Sci.*, 20, 1147 (1980).

40. R. Khanna and N.A. Peppas, *AIChE Symp. Ser.*, 218, 185 (1982).

41. N.A. Peppas, In Proceedings of the Third Wisconsin Update Conference: Packaging, University of Wisconsin Extension Services in Pharmacy, Madison, 1983.

42. W.A. Strickland and M. Moss, *J. Pharm. Sci.*, 51, 1002 (1962).

43. K. Ito, S. Kaga, and Y. Takeya, *Chem. Pharm. Bull.*, 17, 1134 (1969).

44. A.T.M. Serajuddin, P. Sheen, M.A. Augustine, *J. Pharm. Sci.*, 75, 62 (1986).

45. C.M. Bond, K.A. Lees, and J.L. Packington, *The Pharm. J.*, 205, 210 (1970).

46. J.H. Bell, N.A. Stevenson, and J.E. Taylor, *J. Pharm. Pharmacol.*, 25 Suppl., 96P (1973).

47. P. York, *J. Pharm. Pharmacol.*, 33, 269 (1981).

48. K.D. Ross, *Food Technol., Champaign*, 29, 26 (1975).

49. J. Chirife, *J. Food Technol.*, 13, 417 (1978).

50. K.W. Lang and M.P. Steinberg, *J. Food Sci.*, 45, 1228 (1980).

51. K.W. Lang and M.P. Steinberg, *J. Food Sci.*, 46, 670 (1981).

52. K.W. Lang and M.P. Steinberg, *J. Food Sci.*, 46, 1450 (1981).

53. L. Chuang and R.T. Toledo, *J. Food Sci.*, 41, 922 (1976).

54. R.S. Norrish, *J. Food Technol.*, 1, 25 (1966).

55. H. Salwin, *Food Technol.*, 13, 594 (1959).

56. H. Salwin and V. Slawson, *Food Technol.*, 13, 715 (1959).

57. L. Greenspan, *J. Res. N.B.S.*, 81A, 89 (1977).

58. L.B. Rockland and S.K. Nishi, *J. Food Technol.*, 34, 43 (1980).

59. P.W. Winston and D.H. Bates, *Ecology*, 41, 232 (1960).

60. R.H. Stokes and R.A. Robinson, *Ind. Eng. Chem.*, 41, 2013 (1949).

61. J.A. Troller and J.H.B. Christian (eds.), Water Activity and Food, Academic Press, New York, 1978, p.15.

62. Y.K. Sung, In Interaction of Water with Hydrophilic Methacrylate Polymers, Ph.D. Thesis, University of Utah, 1977.

63. "Solutions for Maintaining Constant Humidity", Lange's Handbook of Chemistry, 9th ed., Handbook Publishers, Inc., Sandusky, Ohio, 1956, pp. 1420-1422.

64. H. Nyqvist, *Int. J. Pharm. Tech. and Prod. Mfr.*, 4, 47 (1983).

65. J.R. Adams and A.R. Meez, *Ind. Eng. Chem.*, 21, 305, (1929).

66. G. Edgar and W.O. Swan, *J. Am. Chem. Soc.*, 44, 570 (1922).

67. M.J. Kontny, G.P. Grandolfi, and G. Zografi, *Pharmaceutical Research*, 1987, in press.

68. J.C. Callahan, G.W. Cleary, M. Elefant, G. Kaplan, T. Kensler, and R.A. Nash, *Drug Dev. Ind. Pharm.*, 8, 355 (1982).

69. R.E. Gordon, G.E. Peck, and D.O. Kildsig, *Drug Dev. Ind. Pharm.*, 10, 833 (1984).

70. A. Mitrevej and R.G. Hollenbeck, *Pharm. Tech.*, 10, 48 (1982).

71. D.E. Wurster, G.E. Peck, and D.O. Kildsig, *Starch*, 36, 294 (1984).